Journal of Soils and Sediments
https://doi.org/10.1007/s11368-023-03560-5

SOILS, SEC 3 • REMEDIATION AND MANAGEMENT OF CONTAMINATED OR DEGRADED LANDS • RESEARCH ARTICLE

A comparison of $^{210}Pb_{xs}$, ^{137}Cs, and Pu isotopes as proxies of soil redistribution in South Spain under severe erosion conditions

A. Peñuela[1] · S. Hurtado[2] · V. García-Gamero[1] · J. L. Mas[3] · M. E. Ketterer[4] · T. Vanwalleghem[1] · J. A. Gómez[5]

Received: 22 February 2023 / Accepted: 21 May 2023

Abstract

Purpose The use of fallout radionuclides as proxies for the study of soil redistribution processes in semiarid environments of Southern Spain has been restricted to ^{137}Cs. The potential and limitations of alternative proxies such as $^{239+240}Pu$ and $^{210}Pb_{xs}$ should be explored given the expected constrains imposed by the features of the study area.

Materials and methods Four soil and one sediment cores were collected in a highly eroded area to test the feasibility of these proxies under demanding conditions. The use of gamma spectrometry and ICP-MS did allow exploring the potential of $^{210}Pb_{xs}$ and Pu isotopes against the well-established tracer, ^{137}Cs. The activity ratios $^{239+240}Pu/^{137}Cs$ were explored to evaluate the previous evolution of the sampling sites. Soil redistribution rates were estimated using the model MODERN.

Results and discussion Despite all the profiles showed intense perturbation, Pu isotopes showed the highest potential thanks to higher sensitivity and sample throughput. The deviations of $^{239+240}Pu/^{137}Cs$ inventory ratios (0.012–0.158) from the global fallout average (0.026 ± 0.003) suggest that the sediment core was a deposition site involving alternate episodes of topsoil removal and incorporation from different sources. The calculated erosion rates ranged 34–43 t ha^{-1} $year^{-1}$, being in good agreement for ^{137}Cs and $^{239+240}Pu$. $^{210}Pb_{xs}$ was not used due to low-quality data.

Conclusions The use of Pu as a tracer of soil redistribution processes in semiarid areas seems to be promising even under severe erosion conditions. The use of $^{210}Pb_{xs}$ is not recommended in this area due to its low concentration.

Keywords Isotopes · Soil redistribution · Severe erosion conditions

1 Introduction

In the EU countries of the Mediterranean basin, more than 200,000 km^2 of land is under high risk of soil erosion (Griesbach et al. 1997). Andalusia (South Spain) is one of the most vulnerable areas to water erosion (De La Rosa et al. 1996; García-Ruiz 2010) due to a combination of particularly low vegetation cover, land use types, and high rainfall erosivity (Kosmas et al. 1997; Koulouri and Chr 2007; Panagos et al. 2015) and soil erodibility (Panagos et al. 2014) together with a varied history of land management (García-Ruiz et al. 2013). These factors together with an increasing agriculture intensification produce important both on-site, e.g., reduction of fertile soil, and off-site impacts, e.g., eutrophication of water bodies (Montgomery 2007).

Determining past soil erosion rates over time scales that encompass at least several decades can provide a better insight into long-term trends in soil erosion impacts. Moreover, reconstructed soil erosion rates at appropriate temporal and spatial scales can be used to validate/evaluate soil erosion models (Lang and Bork 2006) which can then be used to predict future impacts and to define and evaluate

Responsible editor: Shiming Ding

Highlights
- The suitability of 210Pbxs, 137Cs, and Pu isotopes to estimate soil loss rates in South Spain is compared.
- 239+240Pu/137Cs inventory ratios allowed the identification of severe soil depth losses.
- Estimated soil loss rates are consistent with published results under similar conditions.
- Pu and Cs concentrations showed similar results, but Pu showed a better performance in terms of analytical sensitivity and sample throughput.

Extended author information available on the last page of the article

Published online: 01 June 2023

mitigation strategies. In Andalusia, several experimental studies based on yearly monitoring have determined soil loss rates at the plot scale (Francia Martínez et al. 2006; Gómez et al. 2009a, b, 2018) and catchment scale (Taguas et al. 2009, 2013; Gómez et al. 2014). However, these records do not exceed a decade in duration, being a notable exception the study carried out by Mabit et al. (2012) who used fallout radionuclides (FRN), in particular ^{137}Cs, to estimate the average soil loss rates since the 1950s.

FRN provide spatially distributed information on soil and sediment redistribution (Dercon et al. 2012). This proxy assumes that these radionuclides are supplied either by dry or wet supply via local or global fallout. Then they strongly bind to surface soil. In this way, their redistribution across a landscape is mainly driven by the same processes responsible for the soil redistribution. The proxy is applied in relative terms; hence, the FRN inventories at the sampled site are compared to those of reference sites. This allows estimating redistribution rates in terms of eroded or deposited mass per surface unit and time unit. One of the main advantages of this approach is that long-term monitoring of experimental fields is not required, resulting in relatively high benefit/cost ratios (Dercon et al. 2012; Allewell et al. 2017).

Among the different FRN, ^{210}Pb ($T_{1/2}=22.3$ years) is a naturally occurring nuclide. Its parent nuclide, ^{222}Rn, exhales into the atmosphere, where it decays to ^{210}Pb, and it is then deposited in the soil as fallout in excess, $^{210}Pb_{xs}$. $^{210}Pb_{xs}$ can provide information about processes occurring within a time-lapse up to 150 years (Mabit et al. 2014). On the other hand, ^{137}Cs ($T_{1/2}=30.1$ years), ^{239}Pu ($T_{1/2}=24{,}110$ years), and ^{240}Pu ($T_{1/2}=6563$ years) are artificial nuclides that were introduced into the environment during the Cold War era, so they may provide information regarding processes lasting up to 55–60 years (Mabit et al. 2018).

The use of FRN in Andalusia has been extremely limited and mainly based on the use of ^{137}Cs (Mabit et al. 2012; Ballais et al. 2013). However, the use of ^{137}Cs as a proxy for soil redistribution is hampered by biogeochemical constrains, rapidly decreasing environmental concentrations due to its short half-life and the accidents of Chernobyl and Fukushima nuclear power plants that injected additional ^{137}Cs signals (see, e.g., Parsons and Foster 2011, 2013; Mabit et al. 2013). Additionally, ^{137}Cs and $^{210}Pb_{xs}$ are usually measured by gamma spectrometry, which is characterized by having a relative high detection limit and low sample throughput (for example, in the conditions provided in Sect. 2.4, 0.5–1 sample per day and detector).

In last years, Pu isotopes have been subject of increasing interest because of their long half-life and the lack of tropospheric sources other than global fallout. The use of mass spectrometric techniques for the measurement of Pu isotopes is a good alternative to radiometric techniques as they can provide high sensitivity and high sample throughput. To this end, techniques such as accelerator mass spectrometry (AMS) and sector focusing inductively coupled plasma mass spectrometry (SF-ICP-MS) have been used (Ketterer and Szechenyi 2008; Tims et al. 2010; Sanders et al. 2016). However, AMS and SF-ICP-MS have very high operational costs, and consequently, they are not an affordable alternative for many researchers. To make it more affordable, the analysis of Pu isotopes has been extended to conventional (quadrupole based) ICP-MS instruments coupled with high efficiency sample introduction systems (Ketterer et al. 2002; Xu et al. 2015).

As far as we know, neither $^{210}Pb_{xs}$ nor Pu isotopes have been evaluated in Andalusia for the analysis of soil erosion/redistribution processes. There are several risks associated to such use from a practical point of view. ^{238}U concentration in natural soils of this region is relatively low in comparison with other regions of Europe (López-Coto et al. 2013); thus ^{210}Pb concentrations are consequently low. Furthermore, the high porosity, scarce soil moisture, and the low frequency of precipitation events suggest that the degree of disequilibrium between ^{210}Pb and its grandparent ^{226}Ra could be small in soils, leading to extremely small concentrations of $^{210}Pb_{xs}$. It also suffers from high uncertainty of measurement results at low activity concentrations (Iurian et al. 2016). In the case of Pu isotopes, as the fallout supply of Pu decreases with latitude, it makes its quantification more difficult in this region than in Northern Europe. Moreover, Pu seems to show a higher binding preference for organic matter in soil (Meusburger et al. 2018), which contents are relatively small in Andalusia. According to Allewell et al. (2017), Pu isotopes have a high potential to become one of the main soil radiotracers; however, more studies are needed to evaluate its suitability under different environmental conditions.

The main goal of this work is to provide background information on the potential suitability of $^{210}Pb_{xs}$ and $^{239+240}$Pu for the study of soil and sediment redistribution in regions whose characteristics establish a priori concerns about their feasibility. The suitability of these techniques was tested by comparing them to other classical indicators of redistribution of soil and sediments such as ^{137}Cs. The main research questions are (1) how detectable are the selected nuclides, (2) what is the order of magnitude of their vertical migration, and (3) how suitable are these nuclides to study soil and sediment redistribution. For this purpose, we have selected a study area with particularly high erosion rates, so the limitations of the techniques can be established under especially demanding conditions. This work would be the first published attempt to use inventories of $^{210}Pb_{xs}$ and Pu isotopes to calculate redistribution rates in this region.

2 Materials and methods

2.1 Study area

The sampling zone was located inside and in the surroundings of the Hornachuelos Natural Park (Fig. 1). The park is located southeast of the Iberian Pyrite Belt and covers an extension of ~ 60,000 ha. The geological settings are mainly characterized by sedimentary and resistant metamorphic rocks with a high degree of metamorphism, mainly consistent in meridional gray–brown soils and rankers developed upon slates, shales, quartzite, and, in general, Paleozoic metamorphic rocks (Moreira 1995). This includes bluish gray loams and slates typical of the South of Sierra Morena mountain range. Dominant soil taxonomy has been characterized as Lythic Xerochrepts (Rosa et al. 1984). Climate has been classified as subhumid Mediterranean, with average temperatures of 19 °C and precipitations within the range of 500–800 mm year^{-1}, mainly concentrated between September and May (Ministerio de Agricultura, Pesca y Alimentación 2008).

Soils are characterized by a scarce development of the edaphic horizons, a low concentration of fertilizer elements, and a strong acidity (Moreira 1995). Farmland is mainly extensive with orchard and cereal production. Vegetation is dominated by typical species of Mediterranean sclerophyllous forest such as holm oak (*Quercus Ilex*), cork oak (*Q. suber*), gall oak (*Q. faginea*), and wild olive tree (*Olea europaea*) (Hidalgo-Fernández et al. 2014). In flatter areas, meadows such as shrubs are dominant. Trees and cereal production is mainly used to feeding cattle and, more recently, animal species destined for big game hunting. At present, more than half the surface of the park is comprised of hunting grounds, leading to certain works that have altered the original ground (installation of fences, reforestation, etc.) (Moreira 1995).

2.2 Soil sampling

Four soil cores and a reservoir sediment core were collected in the study area (Fig. 1, Table 1). Soil core S1 was collected at the base of a hill close to the county road. The collecting

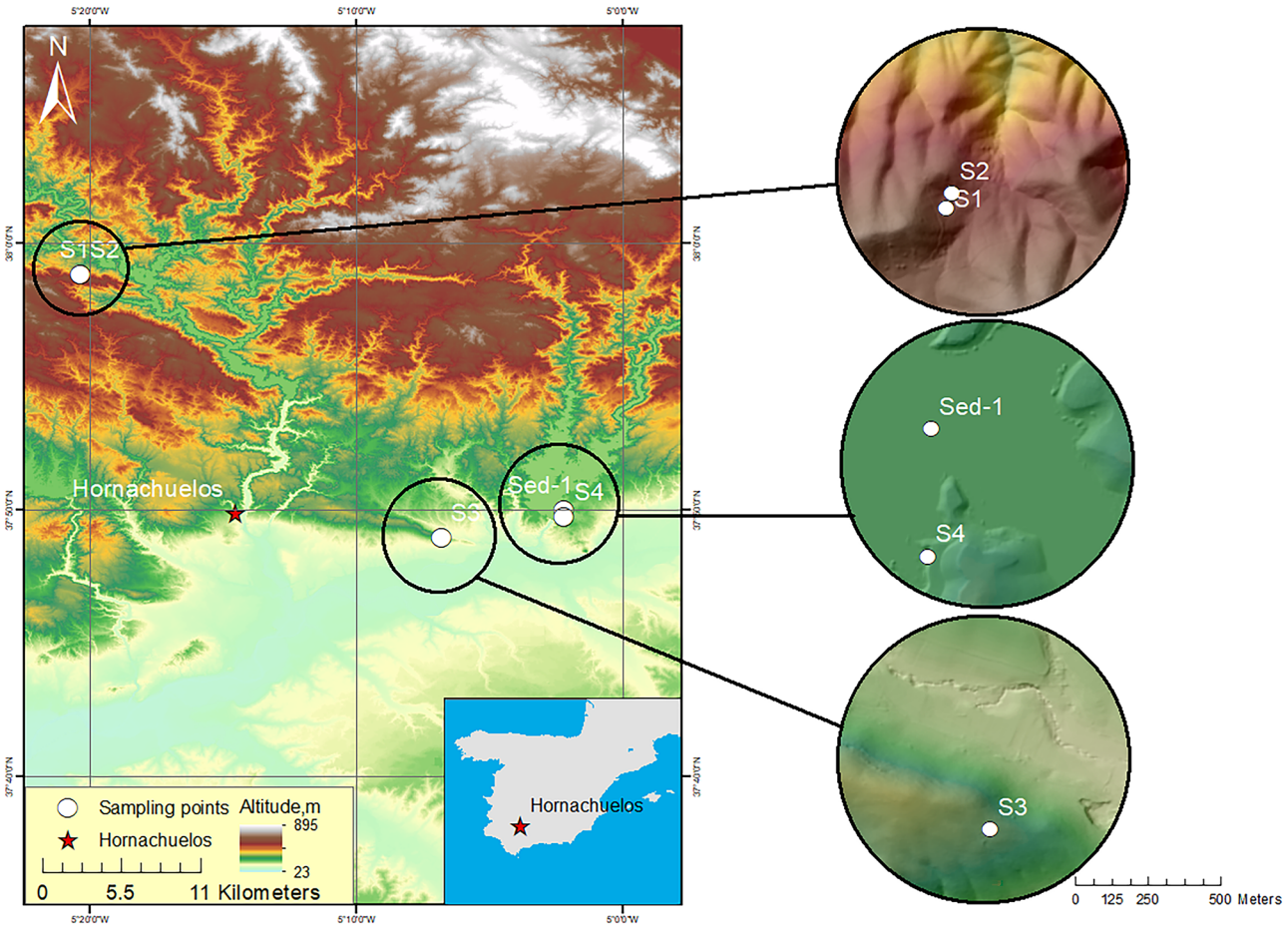

Fig. 1 Location of sampling sites

Table 1 Location, loss on ignition (LOI), and sand:silt:clay percentage of the collected samples. Relative uncertainty for LOI was in the range of 3% for all samples

Core	Coordinates	Depth (cm)	LOI (%)	Sand	Silt	Clay
				Without coarse fraction, %		
S1	37°58′48.66″ N 5°20′23.94″ W	0.0–1.5	7.6	81.2	18.4	0.4
		1.5–3.0	7.1	81.2	18.4	0.4
		3.0–4.5	7.9	68.0	25.7	6.3
		4.5–6.0	7.3	68.0	25.7	6.3
		6.0–7.5	7.0	68.0	25.7	6.3
		7.5–9.0	7.8	68.0	25.7	6.3
		9.0–13.5	8.1	68.0	25.7	6.3
		13.5–16.5	6.6	35.0	50.0	15.0
		16.5–19.5	7.3	56.9	31.5	11.7
		19.5–22.5	7.6	35.4	46.1	18.5
		22.5–25.5	7.5	57.5	32.5	10.0
S2	37°58′48.66″ N 5°20′23.94″ W	0.0–1.0	14.3	52.3	30.9	16.8
		1.0–2.5	13.5	52.3	30.9	16.8
		2.5–4.0	9.3	52.3	30.9	16.8
		4.0–5.5	7.8	52.3	30.9	16.8
		5.5–11.5	7.7	41.7	40.1	18.2
		11.5–17.5	7.4	50.1	35.7	14.2
		17.5–20.5	4.9	66.8	23.8	9.5
		20.5–23.5	7.4	66.8	23.8	9.5
		25.5–26.5	5.9	66.8	23.8	9.5
S3	37°48′56.40″ N 5°6′48.84″ W	0.0–5.0	6.2	57.1	21.7	21.2
		5.0–11.0	8.3	57.1	21.7	21.2
		11.0–14.0	5.1	53.7	21.5	24.8
		14.0–17.0	8.7	59	16.7	24.3
		17.0–20.0	7.5	59	16.7	24.3
		20.0–23.0	9.1	59	16.7	24.3
		23.0–26.0	5.3	51.8	21.3	26.9
S4	37°49′43.94″ N 5°12′12.04″ W	0.0–10.0	7.7	68.9	16.9	14.2
		10.0–13.0	6.8	66.0	18.0	16.1
		13.0–16.0	7.3	63.9	17.0	19.1
		16.0–19.0	7.5	63.1	17.0	19.9
		19.0–22.0	7.5	73.9	12.2	13.9
		22.0–25.0	7.6	53.1	25.2	21.7
		25.0–28.0	7.4	50.5	28.8	20.7

point showed signs of soil accumulation from the upper part of the hill; however it was located near a sharp step, suggesting that both soil erosion and accumulation were possible. S2 was collected at the top of the same hill with no evidences of water stream intrusions, on an a priori basis. Core S3 was collected in a mid-elevation plain of a park near the town of Posadas. The sampling area did show signs of past soil public works such as flattening and removal of the vegetable cover; hence, intense soil mixing should be expected. On the other hand, its location suggested mid-moderate soil erosion. Core S4 was collected in the highest flat top peak of a recreational park close to La Breña reservoir. According to the orography and the presence of vegetation, scarce or null soil removal should be expected. Finally, sediment core Sed-1 was collected in an emerged plain inside the reservoir. The reservoir collects water from Guadiato and Guadalquivir rivers that are being used for irrigation during the dry season. This fact leads to large variations of the accumulated water volume during a year. The steep hills surrounding the main water mass, the presence of 20–30-cm-thick gullies crossing the land hill down to the water body, and the presence of emerged soil masses suggested the potential accumulation of material driven by the runoff during the rain events; hence, this sample site could be considered a sedimentation emplacement on an a priori basis. Sediments act as sinks of radionuclides; hence, what we could expect for this sample is a higher radionuclide inventory than those found in the soil samples. It is worth noting that during the sampling and

the previous exploratory visit to the area, many sites having steeped hills and elevations were surrounded by fences keeping private hunting grounds. Under these conditions, access to many potential sampling sites was impossible, meaning that the sampled sites were not the best possible sampling site candidates but a commitment solution.

Al/Fe hollow tubes, 3.5 cm i.d., and 35–45 cm long were used for sampling. The tubes were slowly unscrewed out with a corner pipe wrench in order to avoid loses from the deeper side, and then they were capped and prepared for transportation to the laboratory. The exploratory nature of this work prevents a thorough application of these techniques on a selected catchment and an adequate application of well-established techniques to select and properly validate reference sites, such as the CHeSs approach (Arata et al. 2017).

2.3 Sample pretreatment and texture analysis

The tubes were sliced into 3–4 cm thickness layers with a reciprocal saw, and the individual samples were oven-dried at 65 °C until constant weight. Thereafter, metallic pieces were removed using a magnet, the stones roots (if any) and man-made tools were removed by hand, and the samples were crushed using a ball mill, with subsequent sifting by a 0.7-mm mesh sieve. Depending on the soil moisture and compaction state of the soil layer, this method allowed us to collect 10–45 g per slice. It is worth indicating that during cores handling at lab, several anomalies appeared such as large holes in the core S2 (apparently animal tunneling, 6–11 cm depth) or finding plastic tools (S3, 5–11 cm depth). That led to a minimum soil recovery for certain soil slices. For those slices, no sample enough was available for gamma spectrometry or Pu isotope analyses.

The sand, silt, and clay contents of soil samples were determined using the Bouyoucos hydrometer method (Gee and Or 2002). First, the soil was oven-dried at 105 °C for 1 day and passed through a 2-mm sieve. Then, < 40 g (or a suitable mass) of soil is taken and mixed with 100 mL of sodium hexametaphosphate solution, for soil aggregate dispersion. After 10 min of soaking the mixture, it is mixed in the dispersion vessel for 5 min. Afterward, the mixture is put into a 1000 mL sedimentation cylinder, and distilled water is added to the 1000 mL line. The suspension is stirred thoroughly by moving it up and down with a brass mixing rod. The timer is started when the mixing rod is removed from the cylinder. Simultaneously, the hydrometer is gently immersed in the suspension, and 30 s later, the hydrometer reading is recorded. After 60 s, a second reading is made. Subsequent readings are taken after 5, 30, and 90 min, and the last reading is taken after more than 8 h. Before the hydrometer was used, a blank reading, including temperature, was performed to correct hydrometer readings. It consists of a cylinder with 100 ml of sodium hexametaphosphate solution added to the 1000 mL line with distilled water. Calculations for sand, silt, and clay percentages, based on the readings at each time interval, were carried out according to Gee and Or (2002).

2.4 Gamma spectrometry

^{40}K, ^{137}Cs, ^{210}Pb, ^{212}Pb (^{228}Th), ^{214}Pb (^{226}Ra), and ^{234}Th (^{238}U) were analyzed at CITIUS (Center for Research, Technology and Innovation of the University of Sevilla, Centro de Investigación, Tecnología e Innovación de la Universidad de Sevilla) by gamma spectrometry using their gamma emissions of 1461, 662, 46.5, 238, 295/352, and 63.3 keV, respectively (Hurtado-Bermúdez et al. 2019). Firstly, the sieved samples were sealed into 80-mL cylindrical beakers and were stored for at least 4 weeks; in this way, ^{226}Ra and their daughters ^{214}Pb and ^{214}Bi reach the radioactive equilibrium condition. Thereafter, the samples were measured in a low-background Canberra HPGe GR-6022 detector (60% relative efficiency) inside a Canberra 777A ultra-low-background lead shield of 15-cm-thick high-purity lead passive shield and a graded liner consisting of low-background tin with a thickness of 1 mm and high-purity copper with a thickness of 1.5 mm. The spectra were analyzed using Canberra Genie 2000 gamma software v3.2. Uncertainties are provided using $k = 1$. Full-energy peak efficiencies (FEPE) were calculated for different energies and an empty beaker using Canberra LabSOCS (Laboratory Sourceless Calibration Software) software. Afterwards, self-attenuation correction factors were calculated using a transmission experiment with non-collimated point sources. The combination of both quantities gave us corrected FEPE and consequently sample activity for any isotope (Hurtado and Villa 2010; Hurtado et al. 2007). The analyses were validated through successful participation in several Monte Carlo intercomparison exercises (Vidmar et al. 2008; Lépy et al. 2012) and also internally through the measurement of several reference materials, IAEA-RGU-1, IAEA-RGTh-1, IAEA-RGK-1, IAEA-444, and IAEA-447. The limits of detection are in the range of 25 Bq kg^{-1} (^{40}K), 1.2 Bq kg^{-1} (^{137}Cs), 8.5 Bq kg^{-1} (^{210}Pb), 3.1 (^{212}Pb), 6.4 (^{234}Th), and 3.5 Bq kg^{-1} (^{226}Ra) (using sample at 22.5–25.5 cm of S1 core).

$^{210}Pb_{xs}$ activity concentration was calculated by subtracting to overall ^{210}Pb activity concentration that of ^{226}Ra (hence, it was assumed that ^{226}Ra and supported ^{210}Pb remain in radioactive equilibrium). Being this approach is quite conventional, certain concerns have been put on it as the radon emanation coefficient is not taken into account. However, the experimental determination of that coefficient is not easy, and the correction is expected to be minimum in soils (Mabit et al. 2014); hence, the correction by ^{226}Ra activity concentration has been used as a commitment approach. When required, statistical tests for homogeneity and variance have been performed using

Statgraphics Centurion 18. All the tests have been performed at the 95% confidence level ($\alpha = 0.05$).

2.5 ^{240}Pu analyses

Pu isotopes were analyzed by ICP-MS after applying a methodology described by Ketterer et al. (2002). Briefly, 10–40 g of each sample was calcined at 550 °C for 12–24 h, and Pu was subsequently leached from the ashes using 16 M HNO_3 (J.T. Beaker™) for 16 h at 80 °C after the addition of ~ 7 pg of ^{242}Pu for the sake of the application of the isotope dilution technique. After filtration and dilution of the filtrate to 8 M HNO_3, Pu was reduced to + IV oxidation state by sequentially adding $FeSO_4$, $NaNO_2$, shaking, and warming at 75 °C for 2 h. Thereafter, 150 mg of the Triskem TEVA extraction chromatography was added to each sample, and shaking was applied for 1 h. The resins were collected in 23-mL LDPE pipettes fitted with a glass wool plug. The resin was sequentially rinsed with 25 mL 2 M HNO_3, 15 mL 8 M HCl, and 10 mL 2 M HNO_3 to remove mass interfering elements such as uranium. Pu was extracted using three sequential elution steps with deionized water, 0.05 M ammonia oxalate, and deionized water again (0.4 mL each one). Under these conditions, the limits of detection for $^{239+240}$Pu were in the range of 5–10 mBq kg^{-1}.

One out of each five samples was used as quality control samples consisting of replicate sample preparation and measurements, blank samples (sandstone samples isolated from radioactive fallout), and the analysis of several aliquots of CRM samples (IAEA-384). Pu contents in this material are quite much higher than the Pu concentrations we expected in the fallout-level samples; hence, every IAEA-384 aliquot was diluted into sandstone (1:350 m:m). The samples were measured at Northern Arizona University (NAU) using a quadrupole ICP-MS (Thermo X2) coupled to an ESI Apex-HF sample introduction system and a 10-roller peristaltic pump (Gilson). Additionally, several of the quality control replicates were prepared and measured at CITIUS using an Agilent 8800 ICP-MS/MS coupled to a CETAC ultrasonic nebulizer. All the quality control samples resulted in values within the expected ones excepting one replicate of the IAEA-384 CRM. This fact was associated to a low chemical yield of plutonium in a sub-batch of samples, meaning that samples with very low chemical yields have not been reported but repeated when possible.

2.6 Use of the $^{239+240}$Pu/^{137}Cs activity ratios and soil mobilization rates

For the cases where both ^{137}Cs and plutonium isotopes were detectable, we have tested the information that could be provided by $^{239+240}$Pu/^{137}Cs activity ratios about the soil evolution. Experimental data (Legarda et al. 2011) showed that the contribution of Chernobyl accident to the ^{137}Cs activity concentrations in soil columns is detectable, but its contribution to the inventories at southern Spanish mainland soils can be neglected against the contribution from global fallout. Regarding plutonium, different evidences showed that atmospheric input due to the Chernobyl accident was minimum and at a very local scale (Alewell et al. 2017). Consequently, the main sources of these nuclides at this latitude are Globall Fallout, and thus, it can be assumed that both radionuclides were supplied at a same pace. A value of activities ratio of 0.026 ± 0.003 has been proposed for global fallout (Hodge et al. 1996) as corrected to July 1998 for the sake of comparison to available data (Alewell et al. 2017), although the different biogeochemistries of these elements can result in deviations from that value as explained below.

The total inventories of Pu and Cs isotopes should be similar to that global fallout value (on what follows, GFV) once provided the soil were undisturbed. We argue, however, that the activity ratios can deviate dramatically from that reference value taking into account that these elements show different biogeochemistry, different migration behaviors, and given the effect of partial soil redistribution. Pu is preferentially associated with colloidal and higher molecular weight materials (Alewell et al. 2017). The deeper migration ability of Pu with respect to Cs has been already shown for Mediterranean soils (Guillén et al. 2015). Therefore, we propose that the activity ratios $^{239+240}$Pu/^{137}Cs cannot be homogeneous through the core profile, although the activity inventory ratios could agree with the GFV for an hypothetical unperturbed soil core.

On the contrary, we would expect that activity ratios show different values deviating from the GFV as a function of depth: (1) the deeper migration ability of Pu regarding Cs would deviate the activity ratios in the deeper part of a core to values higher than the GFV. (2) For upper parts of the core, we could expect by contrast an activity ratio less than GFV. That is exactly what can be derived, for example, from the data of (Guillén et al. 2015).

Subsequently, erosion would remove soil masses (topsoil) with activity ratios less than GFV, producing values higher than GFV in the remaining inventory. Once the eroded soil mass accumulates on top of a previously unperturbed soil core, that location would result in inventory ratios below the GFV (see Graphical abstract, a). Should the same eroded soil mass accumulate on top of weakly eroded soils, the resulting inventories should result in values similar to the GFV (Graphical abstract, b). The studied park is characterized by dramatic changes of the soil uses, meaning that obstacles between a soil source (erosion) and a soil sink (deposition) can appear and disappear with time. And under these conditions, soil sites suffering first weak erosion (resulting

inventory ratios ≥ GFV) and then soil deposition supplied from strongly eroded sites (inventory ratios > GFV) would result in inventory ratios > GFV; i.e., the results at that site should be the result of erosion and deposition episodes.

We will compare this argument with the results provided from erosion and deposition rates as shown below. To do that, MODERN model was used. This model and its potential have been widely described in the literature, as can be seen, for example, in Arata et al. (2016a, b). This model estimates erosion or deposition rates based on the comparison (in the original reference, "alignment") of the total FRN inventory at the sampling site and its depth profile at reference site; in this way, the model returns a solution as a thickness of the soil layer affected by erosion or deposition. The main assumption is that the depth distribution of the selected FRN is the same at the reference and the sampling sites, as it could be expected for any situation where FRN-based models could be applied. Among the main features of MODERN are that its application does not require a transect sampling approach, and, additionally, it does not make any assumption on the shape of the radionuclides profile. The model is available under request to University of Bäsel.

3 Results and discussion

3.1 Soil cores

The activity concentrations obtained in the soil samples for ^{40}K, ^{226}Ra, and ^{210}Pb are shown in Figs. 2, 3, and 4, respectively. The data about the erosion proxies $^{210}Pb_{xs}$, ^{137}Cs, and $^{239+240}$Pu are shown in Table 2. Additional information (in detail values of ^{210}Pb, ^{226}Ra, ^{212}Pb, and ^{234}Th activity concentrations) are provided as supplementary material (Table S1).

The analyzed radionuclides felt below their corresponding limits of detection in a large proportion of the samples: ^{137}Cs, $^{210}Pb_{xs,}$ and $^{239+240}$Pu were undetectable in 69%, 62%, and 54% of the soil and sediment analyzed samples, respectively. This finding is not surprising as the

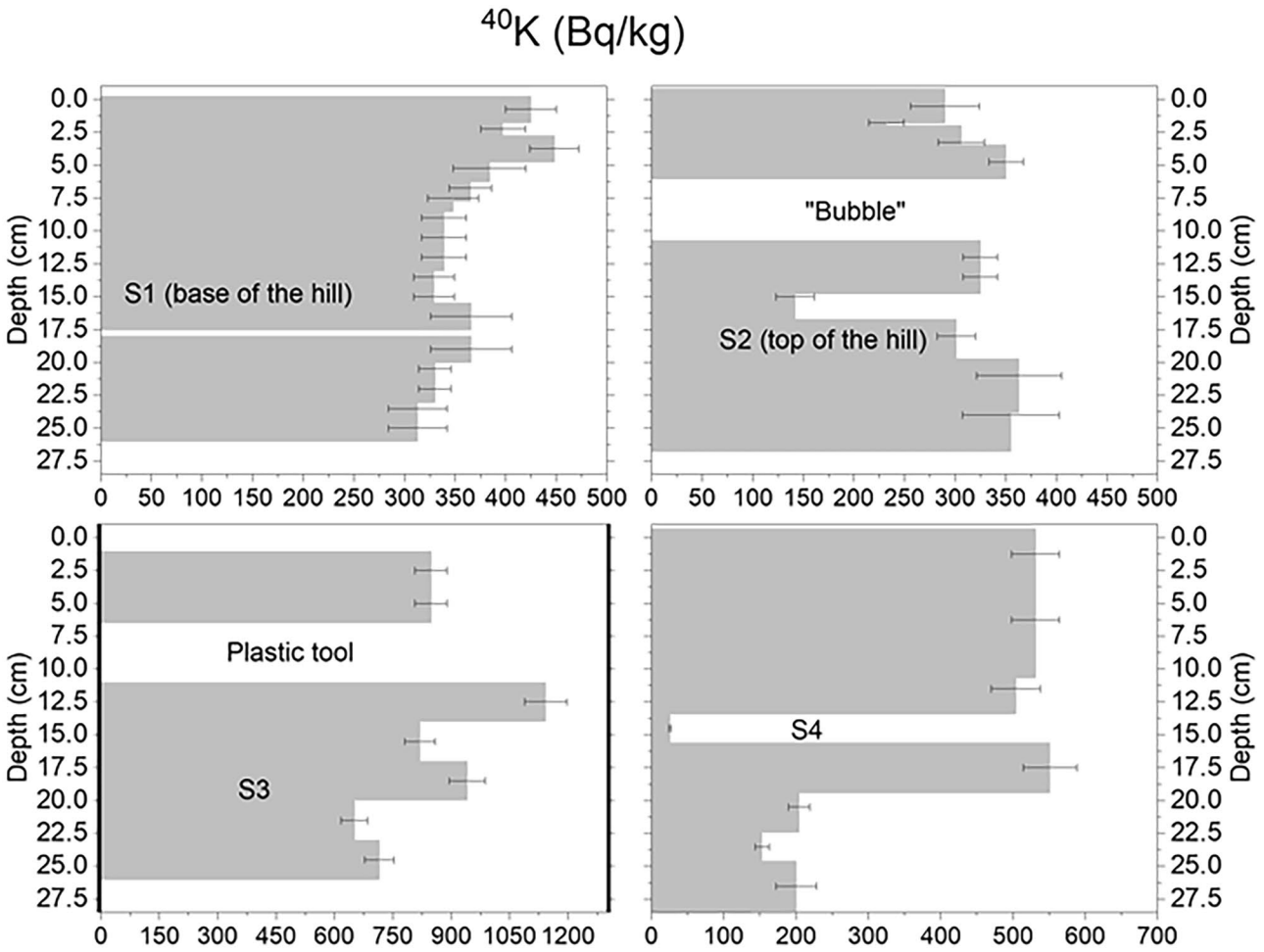

Fig. 2 Activity concentration profiles of ^{40}K in the sampled soils

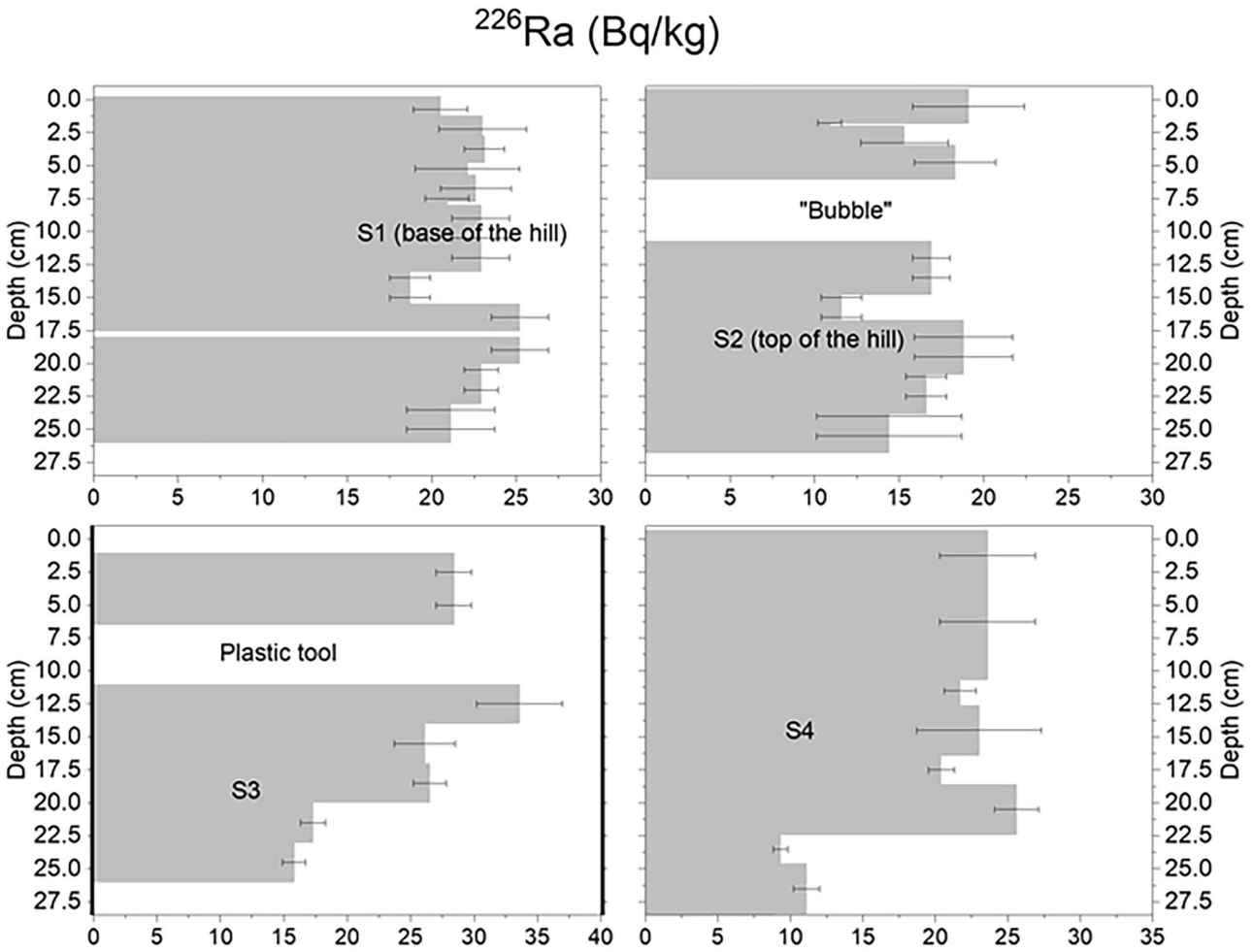

Fig. 3 Activity concentration profiles of ^{226}Ra in the sampled soils

area of study was chosen for the expected high erosion rates (16–70 t ha^{-1} year^{-1}) (Ministerio de Agricultura, Pesca y Alimentación 2008). When the artificial radionuclides were detected, their activity concentrations were within the same order of magnitude than values published for Spanish soils. For example, ^{137}Cs activity concentrations ranged from 1.2 to17.2 Bq kg^{-1}, which are in agreement with values reported in the SW of Spain (Vaca et al. 2001; Mabit et al. 2012). Regarding Pu isotopes, the detected activity concentrations ranged 10.4–365 mBq/kg, which are similar to values found at Southern Spain salt marshes soils (Gascó et al. 2006) or Mediterranean forest soils (Guillén et al. 2015). These facts suggest that the lack of detection is related to intense soil mixing and removal processes.

3.1.1 Natural radionuclides

^{40} K has a relatively constant isotope abundance of potassium in nature (~0.012%), and it forms part of the rock matrix as feldspar and muscovite. However, this element is also supplied with fertilizers; it can be dissolved in environmental water and can be taken up by plant roots through ion channels and specific carriers (Schlesinger 2021). What we could expect is that ^{40} K activity concentrations were nearly constant below the O-horizon and that its concentration varies between sampling points according to the soil composition.

In general, the order of magnitude of the ranges of activity concentration found in the four soil cores (142–1142 Bq kg^{-1}) was in good agreement with data collected at similar latitudes in Spain (Vaca et al. 2001), with the median and ranges proposed for Spain (UNSCEAR 2000) and with the values that could be calculated from the potassium element concentrations published in FOREGS geochemical database for this region (Salminen 2006). These ranges are, furthermore, below the European median. However, several interesting features appeared. The range of variations with depth found in cores S2–S4 (20–48%) was noticeably higher than of S1 (12%) and much higher than those found in other studies in Southern Spain (Mabit et al. 2012). The ^{40} K depletion found at the top of the hill could

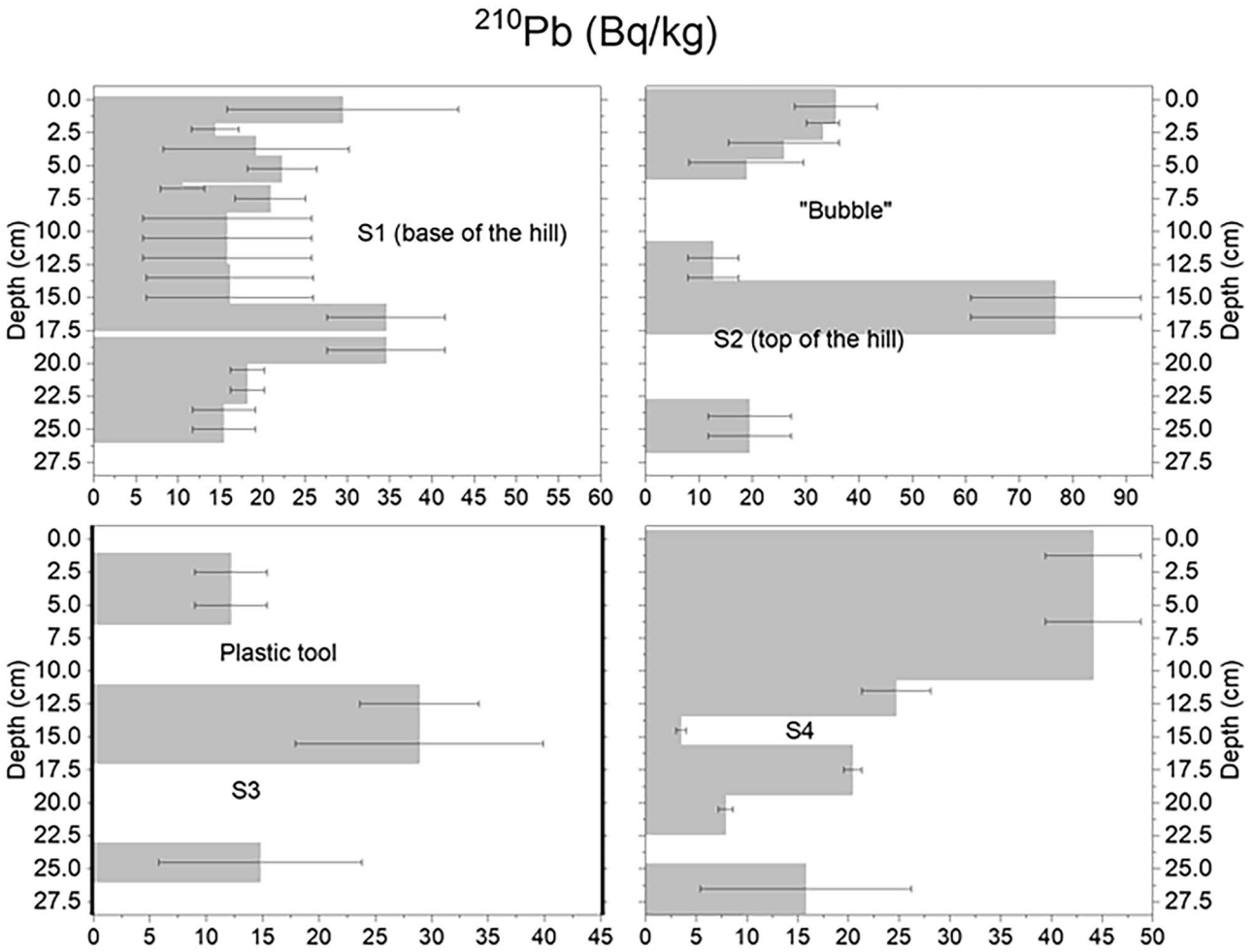

Fig. 4 Activity concentration profiles of ^{210}Pb in the sampled soils

indicate that upper soil layers could have been removed, or, alternatively, that the base of the hill accumulated a part of the potassium supplied either by dead leafs from vegetation or by soil masses supplied from some nearby locations. The fact that ^{40} K activity concentrations in the mid-lower part of core S1 were similar to those of the top of the hill suggests that this last hypothesis could be a plausible one. The fact that the maximum activity concentrations found in core S3 was more than twice those collected in cores S1 and S2 is not surprising as it is reflecting the heterogeneities of the sampling area. On the other hand, the small activity concentration found in the middle of the S4 core cannot be explained by an experimental artifact, so we argue that this layer contained a different soil matrix. This hypothesis is supported by the lack of detection of other natural radionuclides (^{212}Pb and ^{234}Th) and by certain changes in the sand:silt:clay ratio of the soil (Table 1).

Supplementary data provided in Table S1 shows that the concentrations of ^{212}Pb (^{228}Th) and ^{234}Th (^{238}U) are within similar order of magnitudes to median background values calculated for Spanish soils (UNSCEAR 2000) and below world-scale medians. For every soil core, the activity concentrations are within the same order of magnitude inside the uncertainty intervals, although certain heterogeneities of the representative values lead to ranges of variation of 14–50% for ^{212}Pb and 21–82% for ^{234}Th. This internal variability suggests that the soil cores reflect certain mixing between different soil masses. This fact could be associated to natural processes such as runoff and soil deposition as expected for core S1, but it is also compatible with the addition of successive additions of soil layers from different sources with intense compaction as could be expected for core S3.

^{210}Pb was detectable in almost all samples, being activity concentrations within the range 8–77 Bq kg^{-1} (Fig. 4). Excepting a few values in core S2, this range agrees with values previously published for surface unpolluted soils at similar latitudes of Southern Spain (Bolívar et al. 1995; Gascó et al. 2006), in the first case assuming that both ^{210}Pb and ^{210}Po are in equilibrium in the soil system. ^{226}Ra (Fig. 3) was also detectable in almost all the samples, and

Table 2 Activity concentrations found for $^{210}Pb_{xs}$, ^{137}Cs, and $^{239+240}Pu$ in soil cores. N.D: not detected. N.M.: not measured

Core	Depth range (cm)	$^{210}Pb_{xs}$ (Bq kg^{-1})	^{137}Cs (Bq kg^{-1})	$^{239+240}Pu$ (mBq kg^{-1})	$^{239}Pu/^{240}Pu$
S1	0.0–1.5	9 ± 14	N.D	65 ± 14	0.22 + 0.06
	1.5–3.0	N.D	N.D	42.1 ± 6.3	0.19 + 0.04
	3.0–4.5	N.D	N.D	N.D	
	4.5–6.0	0.2 ± 5.1	N.D	N.D	
	6.0–7.5	N.D	N.D	N.D	
	7.5–9.0	N.D	N.D	N.D	
	9.0–13.5	N.D	N.D	N.D	
	13.5–16.5	N.D	N.D	N.D	
	16.5–19.5	9.4 ± 7.2	N.D	N.D	
	19.5–22.5	N.D	N.D	N.D	
	22.5–25.5	N.D	N.D	N.D	
S2	0.0–1.0	16.5 ± 8.4	17.2 ± 0.9	294 ± 46	0.15 + 0.03
	1.0–2.5	22.3 ± 3.2	9.9 ± 1.3	145 ± 50	0.15 + 0.08
	2.5–4.0	11 ± 11	4.3 ± 0.4	N.D	
	4.0–5.5	N.D	1.9 ± 0.9	N.D	
	5.5–11.5	N.D	N.D	N.D	
	11.5–17.5	65 ± 16	N.D	N.D	
	17.5–20.5	N.D	N.D	N.D	
	20.5–23.5	N.D	N.D	N.D	
	25.5–26.5	5.1 ± 8.9	N.D	N.D	
S3	0.0–5.0	N.D	1.2 ± 0.3	138 ± 23	0.17 + 0.04
	5.0–11.0	N.M	N.M	N.M	
	11.0–14.0	N.D	N.D	78 ± 45	0.14 ± 0.10
	14.0–17.0	3 ± 11	N.D	23.5 ± 7.2	0.17 ± 0.07
	17.0–20.0	N.D	N.D	37.4 ± 4.9	0.21 ± 0.04
	20.0–23.0	N.D	N.D	N.D	
	23.0–26.0	N.D	N.D	N.D	
S4	0.0–10.0	20.5 ± 5.7	3.4 ± 1.3	252 ± 11	0.19 ± 0.01
	10.0–13.0	3.1 ± 3.6	4.4 ± 1.6	230 ± 13	0.18 ± 0.01
	13.0–16.0	N.D	N.D	224.9 ± 9.1	0.21 ± 0.02
	16.0–19.0	N.D	13.4 ± 4.7	362 ± 102	0.19 ± 0.01
	19.0–22.0	N.D	N.D	N.D	
	22.0–25.0	N.D	N.D	14.6 ± 7.4	0.16 ± 0.10
	25.0–28.0	5 ± 10	N.D	10.4 ± 2.9	0.18 ± 0.07

the range of the found activity concentrations, 9–34 Bq kg^{-1}, also agrees with the values found in surface forest soils of the South of Spain (Vaca et al. 2001). The ranges of ^{226}Ra activity concentrations cover the average background values established for the country (UNSCEAR 2000), being the maximum below the world-scale median.

For every soil core, the range of variation of ^{226}Ra activity concentrations was 8, 19, 28, and 33% for cores S1 to S4, respectively. The internal variability found for cores S2–S4 seems to be incompatible with unperturbed profiles showing nearly constant activity concentration with depth, like those shown in other parts of Spain; see, e.g., Mabit et al. (2012) and Navas et al. (2017). The variability found for ^{210}Pb was much higher than that of ^{226}Ra: 36, 67, 42, and 60% for cores S1 to S4, respectively. This finding was expected given that the overall activity concentration results from the combination of two sources (in situ and in excess). However, the most remarkable feature of all the ^{210}Pb profiles was the fact that none of them did follow the typical unperturbed core profile. This one typically shows a maximum near the top associated with what should be a continuous atmospheric supply of this radionuclide. On the contrary, several layers had relatively homogeneous activity concentrations, and sometimes detectable activity concentrations were found below layers with undetectable activity concentrations. Furthermore, the activity concentrations of ^{226}Ra were, sample per sample, quite similar to those of ^{210}Pb. Consequently, as shown in Table 2, the number of samples having $^{210}Pb_{xs}$ activity concentration higher than zero was extremely small.

The lack of $^{210}Pb_{xs}$ at the upper part of S1 and S3 and its presence in certain deeper layers such as those detected in cores S1 and S2 can be explained by a combination of intensive removal of the upper part of the soil profiles removing $^{210}Pb_{xs}$-rich soil layers and the deposition of soil from neighbor sources. Average values of atmospheric fluxes of ^{210}Pb in Southern Spain coastal regions have been estimated in ranges of 50–60 Bq m^{-2} $year^{-1}$, while in Northern Spain, they reached 133 Bq/m^2 (Lozano et al. 2011, 2013; Sánchez-Cabeza et al. 2007). Additionally, low contents in organic matter, low pH, or small precipitation could lead to a decreased retention of the atmospherically supplied ^{210}Pb in the soil particles (Meusburger et al. 2018). Combining these facts to low mountain climatology and the subsequent air mass transport in the west-to-east direction, it could be expected that the local supplies of $^{210}Pb_{xs}$ to the topsoil were relatively scarce, even below the 15–25 Bq kg^{-1} level that has been characterized as typical of unsaturated Mediterranean soils (Abril et al. 2018).

In any case, certain doubts arise regarding the suitability of $^{210}Pb_{xs}$ as a potential soil erosion proxy in this region. Similar limitations for the use of this proxy in certain scenarios have been argued by Mabit et al. (2014).

3.1.2 ^{137}Cs

As for $^{210}Pb_{xs}$, ^{137}Cs was detected just in a few samples of every core (0, 4, 2, and 3 layers for cores S1 to S4, respectively). It is worth mentioning that it was not detected in any layer of the core S1, similar to $^{210}Pb_{xs}$, a fact suggesting the removal of the upper soil layers in this ground. The core S2 (top of the hill) shows, opposite to $^{210}Pb_{xs}$, a certain accumulation of ^{137}Cs in the top part of the core, being undetectable below 5.5 cm. Cores S3 and S4, on the other hand, were characterized by a small proportion of samples where ^{137}Cs could be detected including the top of the cores. Furthermore, it was also detected in deep layers despite the fact it could not be detected in many intermediate layers. These facts are again incompatible with an unperturbed profile.

The detected activity concentrations that have been found in this work cover the range 1.2–17 Bq kg^{-1}. This range is comparable to values found in other points of Southern Spain (Vaca et al. 2001; Gascó et al. 2006; Mabit et al. 2012; Guillén et al. 2015). The dependence of the range of concentrations with depth and with the different pluviometry regimes (Legarda et al. 2011) suggests comparing inventories rather than concentrations, as shown in Sect. 3.3.

An immediate question arises regarding the distribution of ^{137}Cs along the different soil cores. In the case of unperturbed soil profiles, it would be expected finding an exponential decrease of activity concentration with a surface or sub-surface maximum. For perturbed soils (for example, after plowing), homogeneous activity concentration with depth may be expected. None of the soil cores fit to any of these two categories. ^{137}Cs was not detected in core S1, while in the case of core S2, as previously mentioned, the core perturbation avoids confirming a possible exponential decrease. However, it could be argued that, assuming an exponential decrease with depth of the ^{137}Cs activity concentration below 5–11 cm depth, its activity concentration could be below the limit of detection of the technique. Indeed, another interesting feature is the fact that no ^{137}Cs could be detected in core S2 below 10 cm depth, a fact that is in strong contrast with previous samplings in the South of Spain (Vaca et al. 2001; Mabit et al. 2012). This difference could be either a consequence of the soil recent evolution or, alternatively, an effect related to the properties of the soils of the sampling sites, such as the contents of clays and karstic leaching (Meusburger et al. 2016). The differences found for ^{137}Cs in cores S1 and S2 could be explained by an accumulation at the hill base of soil masses with a low ^{137}Cs concentration, such as subsoil eroded and transported from gullies (Tims et al. 2010). Indeed, this observation of higher inventories at higher grounds (S2, S4) is consistent with the behavior found for $^{210}Pb_{xs}$.

Soil core S3 showed small activity concentrations in the topsoil and a subsequent decrease below the detection limit below 5 cm depth. A possible explanation of this feature is that the upper layers of the soil have been removed. Under these conditions, this emplacement could be classified a priori as an eroded site. On the contrary, soil profile S4 shows quasi-homogeneous distribution in the upper part with a sharp increase in the middle-lower part of the profile. This profile suggests that the top flat peak where this core was taken was previously submitted to some kind of work involving soil mixing from different origins. The maximum value was quite similar to that found in the top layers of core S2.

3.1.3 Plutonium isotopes

In this work, Pu was detected in 2, 2, 4, and 6 layers of soil cores S1 to S4 (Table 2). In the case of the S1 core, Pu isotopes were the only artificial fallout radionuclides that could be detected, with very small activity concentrations of $^{239+240}Pu$ (42–65 mBq kg^{-1}). In our case, no Pu was detected below the top 3 cm of core S1, and the small concentrations found here in the topsoil are, once again, consistent with the removal processes of the top layers of the ground. The maximum activity concentrations were found at core S4 (up to 350 mBq kg^{-1}). Excepting core S4, Pu isotopes were detected up to a maximum depth in the range of 20 cm. These results agree with previous measurements in Southern Spain salt marshes soils (Gascó et al. 2006) or Mediterranean forest soils (Guillén et al. 2015) but in contrast to results from similar latitudes in Italy (39°N) (Raab et al.

2018). Hence, this finding supports the previous claim for intense upper soil removal.

Fallout Pu concentrations in soils are commonly below activity concentrations of 1 Bq kg^{-1}. For example, concentrations within the range of 50–700 mBq kg^{-1} have been found in the Sila Masif Upland (Italy) (Raab et al. 2018). Similar values have been reported for soils from northern areas in Europe such as the Swiss Alps (50–1000 mBq kg^{-1} (Alewell et al. 2014). Similar higher activity concentrations (~ 10–900 mBq kg^{-1}) have been found in soil cores collected from relatively upper latitudes of Spain (Guillén et al. 2015).

Core S2 showed for Pu isotopes a sharp peak at the top of the core with activity concentrations higher than core S1 (145–295 mBq kg^{-1}). This fact is in agreement with the results found for ^{137}Cs, but then Pu was undetectable below the top of the core in the samples from layers immediately above and below the bioturbation layer (5–11 cm). In core S3, Pu was detectable in the upper layers (similar to ^{137}Cs), but also in several deeper layers, at low to intermediate activity concentrations (less than 150 mBq kg^{-1}). Finally, core S4 showed a relatively homogenous profile within the upper 20 cm. The peak detected at 17.5 cm (same than for ^{137}Cs) cannot be considered significant given the magnitude of the relative uncertainty. Then a drastic drop of activity concentrations appeared in the lower part of the core, being quantification possible at concentrations slightly less than 15 mBq kg^{-1}. Again, these results suggest that Pu and Cs concentrations follow similar but not identical behaviors. Using the Pu + ICP-MS approach allows a better magnitude of the relative uncertainties and a higher sample throughput than using ^{137}Cs + radiometric measurement. This fact emphasizes the advantages of the use of Pu isotopes for the application of the FRN proxy. Indeed, the fact that their quantification was possible in several layers where ^{137}Cs was undetectable seems to suggest that the analysis of Pu could provide more information than ^{137}Cs does. It is also possible that this fact could be coupled to a possible higher vertical migration of Pu relative to Cs (Alewell et al. 2017), as explained below.

3.2 Sediment core

The results obtained from the reservoir sediment core for ^{40} K, $^{210}Pb_{xs}$, ^{137}Cs, and Pu isotopes are shown in Fig. 5. Detailed data of activity concentrations of ^{210}Pb, ^{212}Pb, ^{226}Ra, and ^{234}Th are provided as supplementary material

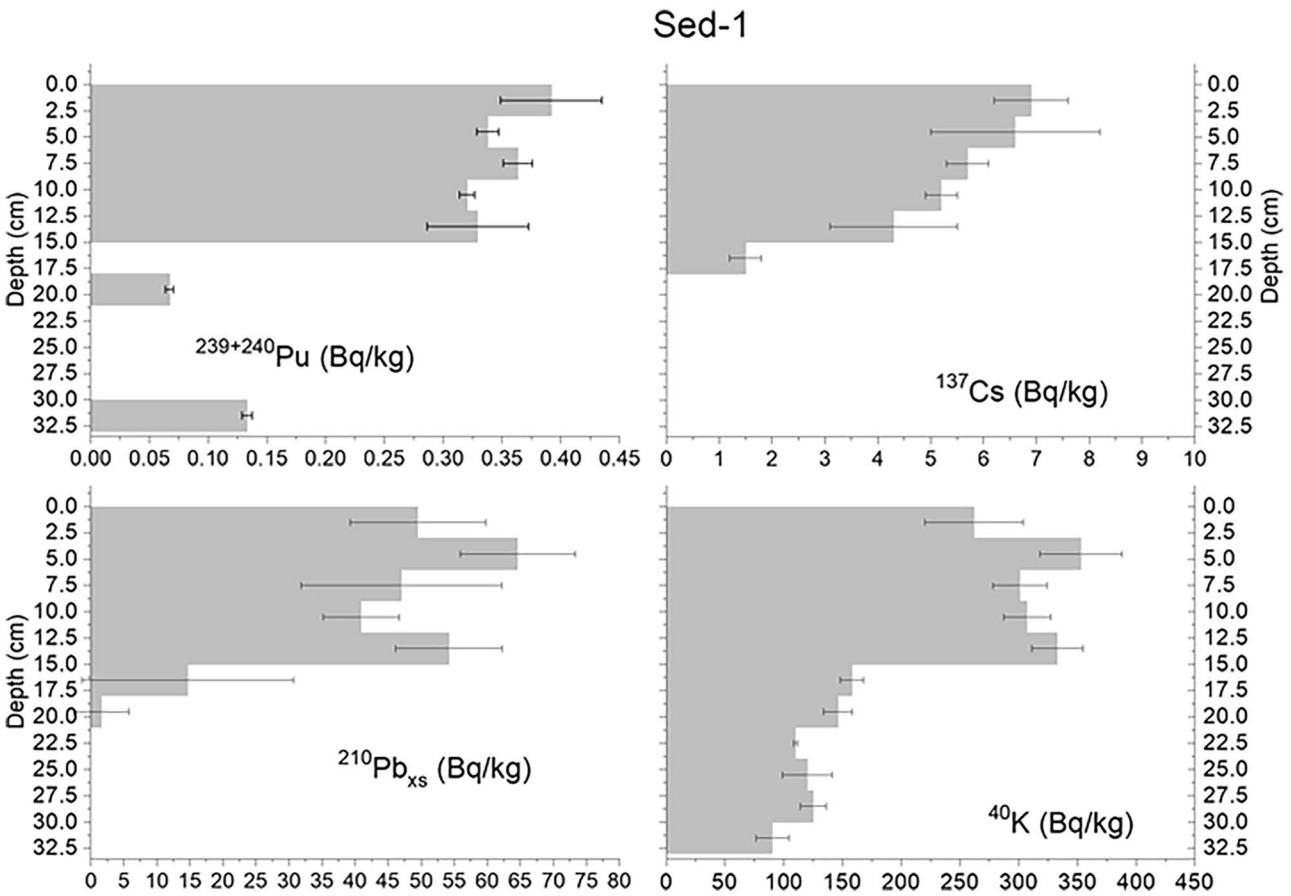

Fig. 5 Activity concentrations found in the reservoir sediment core Sed-1 for ^{40} K, ^{137}Cs, $^{210}Pb_{xs}$, and $^{239+240}$Pu

(Table S2). It can be seen that the activity concentrations of ^{40}K, ^{210}Pb, and ^{212}Pb drop to about half below the 15 cm depth level. This fact suggests that the material deposition evolution in this core has changed through time and involved more than a single source, as explained below. Interestingly, the $^{210}Pb_{xs}$ activity concentrations here reported for the upper part of the core seem to be among the highest values reported in this work (41–65 Bq kg^{-1}). This observation was verified by comparing the populations of $^{210}Pb_{xs}$ activity concentrations for soil samples ($n=10$) and for the upper part of the sediment samples ($n=5$). Medians instead averages were used because the first batch of samples did not correspond to Gaussian distributions. Mann–Whitney *W*-test at a significance level of 5% was applied, revealing that the median in the second batch of data was higher than for the first one, by a factor > 4 (*P*-value = 0.013). $^{210}Pb_{xs}$ on the contrary remained nearly undetectable below the 15 cm depth. $^{210}Pb_{xs}$ activity concentration is nearly homogeneous for the upper part of the core, and this feature is neither compatible with unperturbed soils (where exponential decline should be expected) nor with floodplain soils being developed under a non-episodic accumulation of ^{210}Pb (Abril et al. 2018).

On the other hand, ^{137}Cs was detected in relatively large concentrations (1–7 Bq kg^{-1}) in the upper part of the core until 17.5 cm depth. Something similar was found for Pu isotopes, although detection was possible even at the lowest part of the core (< 150 mBq kg^{-1}) despite they were not detected in intermediate sediment slices.

According to this, our initial hypothesis is that this sediment accumulates materials from different sources after uplands soil removal, downhill transport, and subsequent deposition on the sediment top. Assuming that the isotopic ratio ^{234}Th/^{212}Pb could be representative of the isotopic ratio ^{238}U/^{232}Th, which is a well-known indicator of the origin of particles in sediments (Ivanovich and Harmon 1992), the upper part of the column shows regular values (1.1 ± 0.4–1.8 ± 0.6) but raises to much higher values (3.3 ± 0.6–10.8 ± 4.3) below the 15 cm depth. Hence, the lowest part of the core should contain, possibly, a different substratum from that of the upper part of the core. This hypothesis is supported by the changes in activity concentrations of ^{40}K found below the 15 cm depth. Consequently, this sediment could belong to a depositional and mixing zone. The profile here described seems compatible with two possible scenarios: saturated sediments in the top while the sediment remains submerged (leading to an extremely low ^{222}Rn exhalation) with a scarce capacity for ^{210}Pb redistribution along the sediment column or floodplain soil developed by episodic supplies of material. The lack of $^{210}Pb_{xs}$ below the 15 cm depth layers seems compatible, in turn, with unsaturated soil, where the lack of pore water allows radon exhalation through connected pores and a subsequent depletion of atmospherically supplied ^{210}Pb in the inner layers (Abril et al. 2018). Therefore, we argue that the sediment profile is reflecting an unsaturated soil substrate being covered with surface soil from another source, highly saturated, acting as a natural $^{210}Pb_{xs}$ accumulator.

Summarizing, natural radionuclides such as ^{40}K, ^{212}Pb, and ^{234}Th suggest at least two different sources supplying material to this core with very different signatures, with a clear contrast above and below the 15 cm depth layer and even some intermediate mixing between them. This fact agrees with detectable activity concentrations of ^{137}Cs, $^{210}Pb_{xs}$, and $^{239+240}$Pu above that depth and undetectable levels below that depth. The scenario suggested by the natural radionuclides in the sediment core resulted compatible, on the other hand, with the results found for artificial radionuclides. The retention of ^{137}Cs and $^{239+240}$Pu in a top soil is modulated by erosion processes. As the soil column loses surface masses, where Pu and ^{137}Cs activity concentrations are higher, the inventory of these nuclides decreases. These isotopes subsequently accumulate in another location, acting as a sink. When a soil already depleted in these nuclides suffers additional erosion, this Pu and ^{137}Cs depleted material accumulates on top of an accumulation point. These processes of erosion, runoff transport, and deposition can be extended through many years. It can be the same location than before or not depending upon the existence of abrupt processes such as human-driven soil redistribution. Under these conditions, a same sink position can receive soil mass supplied by two different sources having different levels of retention of FRNs. The lack of detection below the 15 cm depth layer may be explained following two alternative possibilities: (1) the underlying soil could be supplied by an already eroded ground, before the incorporation of additional soil masses. That would define a complex scenario involving alternate, non-continuous episodes of upper soil removal and incorporation (i.e., top soil replacement instead of accretion). (2) This sediment location could act as a sink of soils from different locations having different previous histories. The lower part in the core would correspond to the deposition of soil supplied by gullies, which are depleted in fallout reactive particle nuclides (Tims et al. 2010). The top part of the sediment location should be supplied from topsoil keeping a part of their radionuclide inventories. This last possibility is coherent with the hypothesis depicted above based on the results obtained for $^{210}Pb_{xs}$. The random detection of Pu in several lower layers would be a combined consequence of two different effects: the better performances of ICP-MS for Pu isotope detection over the gamma analysis for ^{137}Cs and the ability of plutonium to be transferred deeper inside the soil/sediment column (Meusburger et al. 2016).

3.3 Inventories

As shown above, the interpretation of data can be complicated by the combination of several factors involving element's biogeochemistry and soil redistribution. From this point of view, a comparison of inventories could help to clarify the net role (source vs. sink) of every location. Figures 6, 7, and 8 summarize the $^{210}Pb_{xs}$, ^{137}Cs, and $^{239+240}Pu$ inventories calculated for the soil and sediment cores. $^{210}Pb_{xs}$ inventories in soil ranged from 0 to 3.33 ± 0.72 kBq m^{-2} with an average of 1.7 ± 0.2 kBq m^{-2} for soils. Gascó et al. (2006) reported 0.1–9.4 kBq m^{-2} in soils of Doñana National Park, being the average 3.9 ± 1.8 kBq m^{-2}. Values of 1.94 ± 0.08 kBq m^{-2} were reported in reference sites at higher latitudes in Spain, NE Spanish Pre-Pyrenees (Gaspar et al. 2013), and different authors have reported inventories of up to 5.4–10.9 kBq m^{-2} at reference sites in different locations around the region of Calabria, Italy (Porto et al. 2012). The inventories found in the soil samples indicate extensive removal of the upper layers of soils at the sampled points. This last possibility suggests in turns that the use of $^{210}Pb_{xs}$ could be compromised despite its successful application in other emplacements having similar climate conditions. On the contrary, the inventory found in the sediment core was noticeably high (9810 ± 1008 Bq m^{-2}). From a qualitative point of view, the different magnitudes of the inventories in soil suggest that the use of $^{210}Pb_{xs}$ could allow discriminating eroded sites (S1 and S3) and depositional sites (Sed-1).

The inventories of ^{137}Cs in soil cores ranged between 0 and 1049 ± 237 Bq m^{-2} (Fig. 9). The maximum value corresponded to core S4, and it overlapped the inventory calculated for the sediment core, 1087 ± 79 Bq m^{-2}. This range of inventories is slightly less than previous data published for reference sites sampled at similar latitudes (Montefrío, Granada, Spain, 37°19′ N, 4°0′ W), having a value of 1.9 ± 0.2 kBq m^{-2} (Mabit et al. 2012), and it is also the same order of magnitude than values predicted for ^{137}Cs deposition with the above-mentioned mean yearly rainfall (1400–1800 Bq m^{-2}) (Legarda et al. 2011). As expected, the values of this work inventories are usually much less than inventories of reference sites belonging to Northern latitudes in Spain; see, for example, Menéndez-Duarte et al. (2009) and Sánchez-Cabeza et al. (2007). On the contrary, just 1570 ± 80 Bq m^{-2} were reported in Pre-Pyrenees lands (Gaspar et al. 2017).

The general trends for ^{137}Cs inventories (Sed-1 ≈ S4 > S2 > S3 > > S1) clearly show that the locations of S3 and S1 suffered an intense removal of the upper soil layers, as suggested in the previous section. In this case the conclusion agrees with that provided by the $^{210}Pb_{xs}$ inventories. On the contrary, S4 inventory was clearly higher than that of S2, while in the case of $^{210}Pb_{xs}$, they were quite similar taking into account the corresponding uncertainty intervals. Furthermore, the use of ^{137}Cs inventories do not allow a

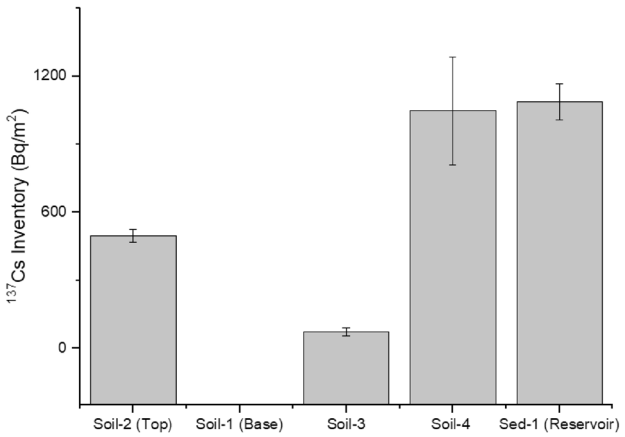

Fig. 7 ^{137}Cs inventories calculated for soil and sediment cores

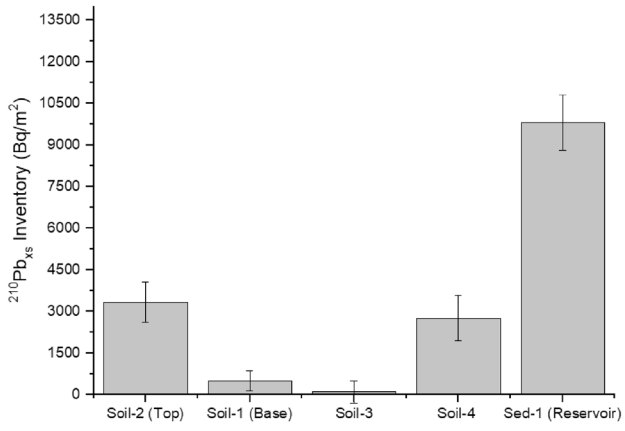

Fig. 6 $^{210}Pb_{xs}$ inventories calculated for the soil cores and the sediment core. Error bars show the associated interval uncertainty after quadratic propagation of all sources within a confidence interval $k = 1$

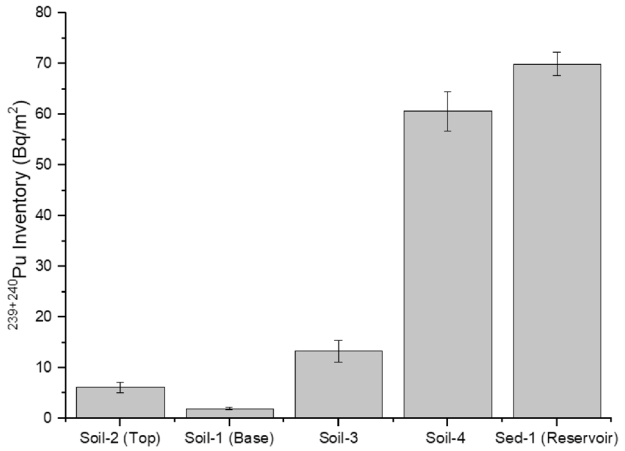

Fig. 8 $^{239+240}Pu$ inventories calculated for soil and sediment cores

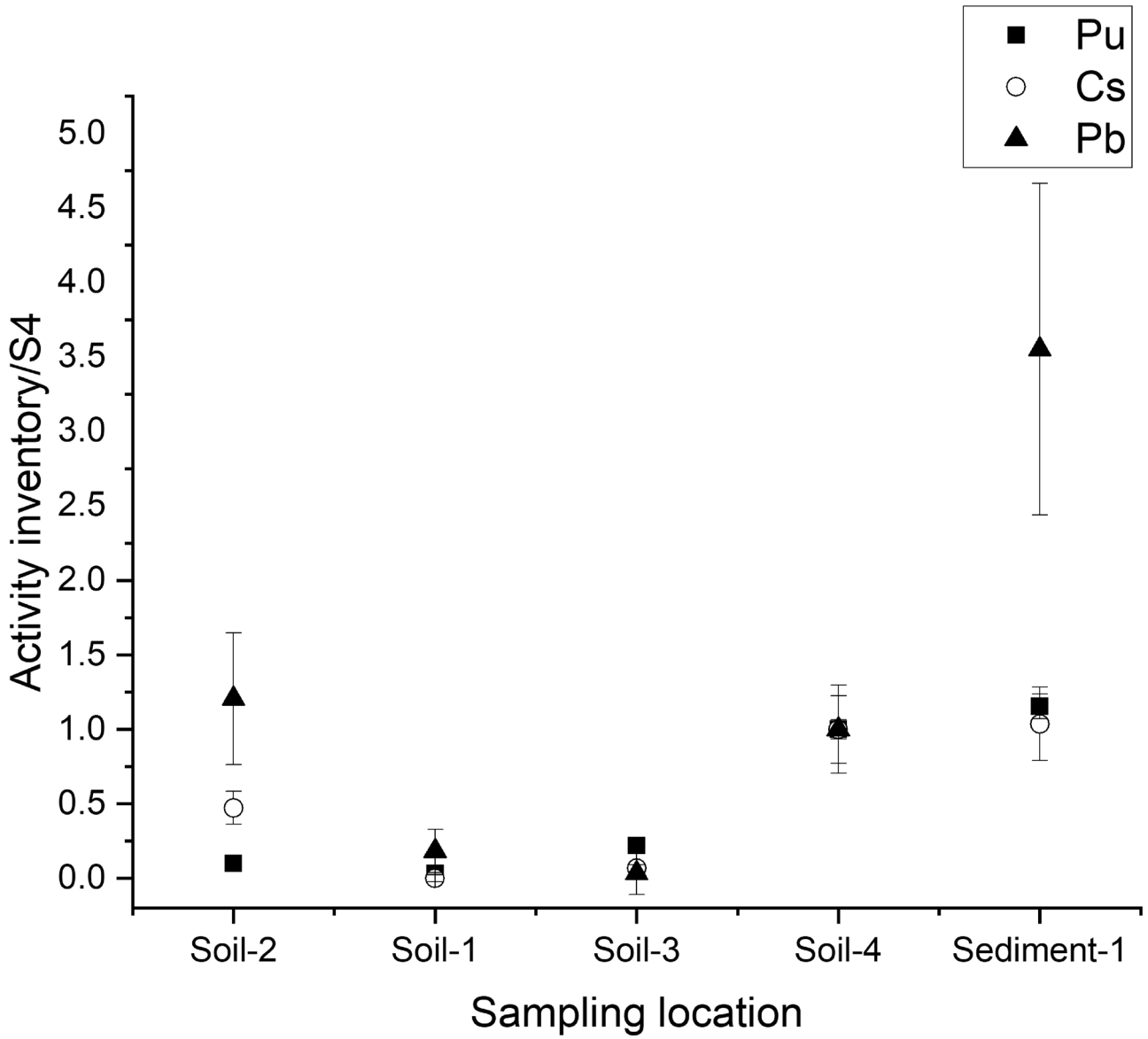

Fig. 9 Normalized inventories of $^{210}Pb_{xs}$, ^{137}Cs, and.$^{239+240}Pu$ calculated for soil and sediment cores. The normalization values are those of core S4

clear identification of Sed-1 emplacement as a deposition site because it was quite similar to that one calculated for S4. This finding is in conflict with the information provided by $^{210}Pb_{xs}$.

Finally, in the case of Pu isotopes, the inventories ranged from 1.9 to 60.6 Bq m^{-2}. Similar to that found for ^{137}Cs, the inventories calculated for S4 and Sed-1 were within the same order of magnitude (60.6 ± 3.9 and 70.0 ± 2.3 Bq m^{-2}, respectively). Using the linear relationship between Pu deposition and average annual rainfall proposed in (Gascó et al. 2006), the expected inventories lie between 40 and 54 Bq m^{-2}, a range that is in good agreement with our maximum values for soils. The availability of data regarding fallout-level Pu inventories of the South of Spain is very scarce. Values from 16.4 Bq m^{-2} (eroded site) to 101.1 Bq m^{-2} (depositional site) have been published for salt marshes soils in Doñana National Park (Gascó et al. 2006). On the other hand, 256.2 Bq m^{-2} was reported at a dam sediment column from SW Spain (Abril et al. 2018), while Chamizo (2009) reported 45–137 Bq m^{-2} in estuarine sediment cores. In this case, the relationship between inventories shows that Sed-1≈S4 > > S3 > S2 > S1.

Location S4 is, in relative terms, a maximum of inventories among the soil cores for both natural and artificial radionuclides. S1 and S3 are clearly revealed as erosion sites. Sed-1 reveals as a potential slight accumulation site, which

is much more pronounced in the case of $^{210}Pb_{xs}$, possibly as a consequence of the reasons explained in Sect. 3.2. The main differences appear for emplacement S2, which is clearly an eroded site according to ^{137}Cs and $^{239+240}Pu$ inventories, but not according to $^{210}Pb_{xs}$ when relative uncertainties are taken into account.

Another derivative of the data here shown relates to the different sensitivity offered by the three approaches used in this work. Such sensitivity should be considered in terms of (1) the ratio of typical order of magnitude of the activity concentration to limit of detection, (2) the relative magnitude of uncertainties for both activity concentrations and inventories, and also (3) the ability to quantify the presence of the nuclides in deeper layers. From these points of view, Pu isotopes seem to be a most remarkable proxy for soil redistributions than $^{210}Pb_{xs}$ or ^{137}Cs. Indeed, the combined use of ^{137}Cs and Pu isotopes can reinforce the discussion of the results, especially when the calculation of erosion rates requires corrections of the estimative values by the soil particle size, as suggested in Meusburger et al. (2016). Otherwise, a systematic overestimation of the soil redistribution rates could be derived due to the preferential transport of small size particles, which are assumed to be enriched in ^{137}Cs regarding Pu isotopes.

Interesting issues appear if $^{239+240}Pu/^{137}Cs$ activity ratios are calculated for the full inventories instead individual samples. S4 reflects an inventories ratio of 0.058 ± 0.014, which agrees quite well with the inventories ratios calculated for soils in Mediterranean forests, 0.063–0.083 (Guillén et al. 2015). We argue that the deeper penetration of Pu regarding Cs can be detected in eroded soils. Removal of surface soil layers leads to inventory ratios above the reference value in the eroded sampling site. This is the situation that we have found for core S3, where the inventory ratio was 0.184 ± 0.055 (z-score = 1.42). If erosion continues deeper than Pu maximum, the resulting inventory ratio decreases, as found for core S2 (0.012 ± 0.002; z-score = −0.92).

The profile of soil S4 did not correspond neither to unperturbed nor plowing profile. On a strict sense, it should not be the best possible option for a reference profile for the sake of calculation of erosion rates. However, the good agreement of ^{137}Cs and $^{239+240}Pu$ inventories at this core with the values found at similar latitudes suggests the possibility to use it in order to evaluate erosion rates on a relative basis. To do that, MODERN was used as explained above. In this case, we did transform the data collected in the profile S4 for Cs and Pu isotopes, with variable slice thickness, into constant 3 cm thickness. The other supplied data were the radionuclide inventories at the sampling locations (S1, S2, S3 and Sed-1). The simulations were not applied to $^{210}Pb_{xs}$ data due to their low quality, in relative terms.

The simulations for ^{137}Cs did reveal integrated soil losses of − 16, − 16, and − 22 cm for soil cores S1, S2, and S3 for the period 1963–2017. For Pu isotopes, the results were in reasonably good agreement with the former results: − 20, − 18, and − 16 cm, respectively. The results obtained for ^{137}C correspond to soil erosion rates in the range of 34, 34, and 41 t·ha^{-1}·year^{-1}, respectively (43, 38 and 34 t·ha^{-1}·year^{-1}, respectively, using Pu isotopes). These values are consistent with RUSLE predictions in the study area (12–65 t·ha^{-1}·year^{-1}); details of the application of RUSLE at this scale (1:400,000) can be found in (Ministerio de Agricultura, Pesca y Alimentación 2008). However, the scale of this approach does not allow obtaining accurate data for the specific coordinates of the sampling points. Similarly, the average erosion rates in the range of 10–40 t·ha^{-1}·year^{-1} for a set of farms located between Bembézar and Retortillo dams were calculated by Alcántara Jurado et al. (2006). In any case, the calculations show erosion rates that can be described as severe, as expected. On the other hand, MODERN predicts two different scenarios for the location of Sed-1 depending upon the used radionuclide. For ^{137}Cs, a slight soil loss is predicted, − 1.2 cm, while for Pu isotopes, a slight deposition rate is predicted (2.8 cm). These differences are certainly the result of the fact that the inventories at S4 and Sed-1 are barely the same for Cs isotopes when the uncertainty bars are considered, although higher resolution was achieved using Pu isotopes.

4 Summary and conclusions

Different soil redistribution markers have been analyzed in soil and sediment cores collected in a region where severe to very severe soil erosion was expected. The limitations of the use of $^{210}Pb_{xs}$ as a proxy for the calculation of soil erosion rates in semiarid environments with high erosion rates have been shown. The exploratory use of Pu isotopes, compared to ^{137}Cs, revealed certain advantages for the former in terms of analytical sensitivity and sample throughput. The collected data suggests intense soil erosion since 1954 to 2012 (34–43 t ha^{-1}·year^{-1}), which are within the order of magnitude proposed through the application of RUSLE. For the collected reservoir sediment core, discrepancies between the data provided by $^{210}Pb_{xs}$ on one hand, and the artificial radionuclides on other hand, can be explained by arguing that the sediment profile was reflecting an unsaturated soil substrate being covered with highly saturated surface soil from another source and acting therefore as a natural $^{210}Pb_{xs}$ accumulator. The use of Pu as a tracer of erosion processes in semiarid areas needs to be further evaluated in future studies at different sites around the world in order to demonstrate how affordable is its use as an universal alternative to the use of ^{137}Cs and $^{210}Pb_{xs}$.

Supplementary Information The online version contains supplementary material available at https://doi.org/10.1007/s11368-023-03560-5.

Acknowledgements The authors want to express their deep acknowledgement to Prof. Jani Ingram (Northern Arizona University) and Prof. Esteban Alonso (University of Sevilla, CITIUS) for the access to the instruments used in this work. In the same way, the authors acknowledge Universität Basel for providing access to the MODERN code and two reviewers for their constructive comments, questions, and suggestions during the revision process of this manuscript.

Funding Funding for open access publishing: Universidad de Sevilla/CBUA. Different parts of this work have been partially founded by the Spanish Ministry of Science, Innovation and Universities (FIS-2015–69673-P; PID2019-109924RB-I00), and by the Research Plan of University of Sevilla (VI PPI-ID SOL2017-9049).

Data availability The data underlying this article will be shared on reasonable request to the corresponding author.

Declarations

Conflict of interest The authors declare no competing interests.

References

Abril JM, San Miguel EG, Ruiz-Canovas C, Casas-Ruiz M, Bolívar JP (2018) From floodplain to aquatic sediments: radiogeochronological fingerprints in a sediment core from the mining impacted Sancho Reservoir (SW Spain). Sci Total Environ 631–632:866–878. https://doi.org/10.1016/j.scitotenv.2018.03.114

Alcántara Jurado AM, Gómez JA, Fereres Castiel E (2006) Evaluación del riesgo de erosión y productividad del olivar en producción integrada (In Spanish). Revista Agropecuaria 75(885):426–433. https://www.miteco.gob.es/ministerio/pags/Biblioteca/Revistas/pdf%5FAgri%2FAgri%5F2006%5F885%5F426%5F433%2Epdf. Accessed 16 Jan 2023

Alewell C, Meusburger K, Juretzko G, Mabit L, Ketterer ME (2014) Suitability of 239+240Pu and 137Cs as tracers for soil erosion assessment in mountain grasslands. Chemosphere 103:274–280. https://doi.org/10.1016/j.chemosphere.2013.12.016

Alewell C, Pitois A, Meusburger K, Ketterer ME, Mabit L (2017) 239 + 240Pu from "contaminant" to soil erosion tracer: where do we stand? Earth Sci Rev 172:107–123. https://doi.org/10.1016/j.earscirev.2017.07.009

Arata L, Alewell C, Frenkel E, A'Campo-Neuen A et al (2016b) Modelling Deposition and Erosion rates with RadioNuclides (MODERN) – part 2: a comparison of different models to convert 239+240Pu inventories into soil redistribution rates at unploughed sites. J Environ Radioact 162–163:97–106. https://doi.org/10.1016/j.jenvrad.2016.05.009

Arata L, Meusburger K, Bürge A, Zehringer M, Ketterer ME, Mabit L, Alewell C (2017) Decision support for the selection of reference sites using 137Cs as a soil erosion tracer. SOIL 3(3):113–122. https://doi.org/10.5194/soil-3-113-2017

Arata L, Meusburger K, Frenkel E, A'Campo-Neuen A et al (2016a) Modelling Deposition and Erosion rates with RadioNuclides (MODERN) - part 1: a new conversion model to derive soil redistribution rates from inventories of fallout radionuclides. J Environ Radioact 162–163:45–55. https://doi.org/10.1016/j.jenvrad.2016.05.008

Ballais JL, Cohen M, Bonté P, Larromanière M, Lefèvre I, Maingre A et al (2013) Hydric erosion in Sierra Magina olive groves (Andalusia, Spain) - prospects for sustainable development. Zeitschrift Fur Geomorphologie 57(1):1–23. https://doi.org/10.1127/0372-8854/2012/0088

Bolívar JP, García-Tenorio R, García-León M (1995) Enhancement of natural radioactivity in soils and salt-marshes surrounding a non-nuclear industrial complex. Sci Total Environ 173(174):125–136. https://doi.org/10.1016/0048-9697(95)04735-2

Chamizo E (2009) Medida de isótopos de Plutonio, 239Pu y 240Pu, mediante espectrometría de masas con aceleradores de baja energía (Ph. D. Thesis dissertation). University of Sevilla (Spain), Sevilla (Spain). Retrieved from https://idus.us.es/handle/11441/15768;jsessionid=EB849CD8EE5DC664B8381255FD2F8E7D?. Accessed 14 Jan 2023

De La Rosa D, Crompvoets J, Mayol F, Moreno JA (1996) Land vulnerability evaluation and climate change impacts in Andalucia, Spain: soil erosion and contamination. Int Agrophys 10(3):225–238

Dercon G, Mabit L, Hancock G, Nguyen ML, Dornhofer P, Bacchi OOS et al (2012) Fallout radionuclide-based techniques for assessing the impact of soil conservation measures on erosion control and soil quality: an overview of the main lessons learnt under an FAO/IAEA Coordinated Research Project. J Environ Radioact 107:78–85. https://doi.org/10.1016/j.jenvrad.2012.01.008

Francia Martínez JR, Durán Zuazo VH, Martínez Raya A (2006) Environmental impact from mountainous olive orchards under different soil-management systems (SE Spain). Sci Total Environ 358(1–3):46–60. https://doi.org/10.1016/j.scitotenv.2005.05.036

García-Ruiz JM (2010) The effects of land uses on soil erosion in Spain: a review. CATENA 81(1):1–11. https://doi.org/10.1016/j.catena.2010.01.001

García Ruiz JM, Nadal-Romero E, Lana-Renault N, Beguería S (2013) Erosion in Mediterranean landscapes: changes and future challenges. Geomorphology 198:20–36. https://doi.org/10.1016/j.geomorph.2013.05.023

Gascó C, Antón MP, Pozuelo M, Clemente L, Rodríguez A, Yañez C et al (2006) Distribution and inventories of fallout radionuclides (239+240Pu, 137Cs) and 210Pb to study the filling velocity of salt marshes in Doñana National Park (Spain). J Environ Radioact 89(2):159–171. https://doi.org/10.1016/j.jenvrad.2006.05.004

Gaspar L, Navas A, Walling DE, Machín J, Gómez Arozamena J (2013) Using 137Cs and 210Pbex to assess soil redistribution on slopes at different temporal scales. CATENA 102:46–54. https://doi.org/10.1016/j.catena.2011.01.004

Gaspar L, Webster R, Navas A (2017) Fate of210Pbexfallout in soil under forest and scrub of the central Spanish Pre-Pyrenees. Eur J Soil Sci 68(3):259–269. https://doi.org/10.1111/ejss.12427

Gee WG, Or D (2002) Particle-size analysis. In: Dane, J., Topp, G.C. (Eds.), Methods of soil analysis. Book Series: 5. Part 4. Soil Science Society of America, USA, pp. 255–293

Gómez JA, Campos M, Guzmán G, Castillo-Llanque F, Vanwalleghem T, Lora Á, Giráldez JV (2018) Soil erosion control, plant diversity, and arthropod communities under heterogeneous cover crops in an olive orchard. Environ Sci Pollut Res 25(2):977–989. https://doi.org/10.1007/s11356-016-8339-9

Gómez JA, Guzmán MG, Giráldez JV, Fereres E (2009b) The influence of cover crops and tillage on water and sediment yield, and on nutrient, and organic matter losses in an olive orchard on a sandy loam soil. Soil Tillage Res 106(1):137–144. https://doi.org/10.1016/j.still.2009.04.008

Gómez JA, Sobrinho TA, Giráldez JV, Fereres E (2009a) Soil management effects on runoff, erosion and soil properties in an olive grove of Southern Spain. Soil Tillage Res 102(1):5–13. https://doi.org/10.1016/j.still.2008.05.005

Gómez JA, Vanwalleghem T, De Hoces A, Taguas EV (2014) Hydrological and erosive response of a small catchment under olive cultivation in a vertic soil during a five-year period: implications for sustainability. Agric Ecosys Environ 188:229–244. https://doi.org/10.1016/j.agee.2014.02.032

Griesbach JC, Ruiz Sinoga JD, Giordano A, Berney O, Gallart F, Rojo Serrano L (1997) PAP/RAC: guidelines for mapping and measurement of rainfall-induced erosion processes in the Mediterranean coastal areas. https://www.fao.org/3/x5302e/x5302e00.htm. Accessed 16 Jan 2023

Guillén J, Baeza A, Corbacho JA, Muñoz-Muñoz JG (2015) Migration of 137Cs, 90Sr, and 239+240Pu in Mediterranean forests: influence of bioavailability and association with organic acids in soil. J Environ Radioact 144:96–102. https://doi.org/10.1016/j.jenvrad.2015.03.011

Hidalgo-Fernández A, Fernández REH, Madueño JAC, Cañete RB (2014) Economic valuation of the recreational use of "Sierra de Hornachuelos" Natural Park (Cordoba, Spain) | Valoración del uso recreativo del Parque Natural Sierra de Hornachuelos (Córdoba, España). Interciencia 39(3):172–179. https://www.interciencia.net/wp-content/uploads/2017/10/172-c-1%C2%BA-HIDALGO-FERNANDEZ-8.pdf. Accessed 21 Jan 2023

Hodge V, Smith C, Whiting J (1996) Radiocesium and plutonium: still together in "background" soils after more than thirty years. Chemosphere 32(10):2067–2075. https://doi.org/10.1016/0045-6535(96)00108-7

Hurtado S, Villa M (2010) An intercomparison of Monte Carlo codes used for in-situ gamma-ray spectrometry. Radiat Meas 45(8):923–927. https://doi.org/10.1016/j.radmeas.2010.06.001

Hurtado S, Villa M, Manjón G, García-Tenorio R (2007) A self-sufficient and general method for self-absorption correction in gamma-ray spectrometry using GEANT4. Nucl Instrum Methods Phys Res A 580:234–237. https://doi.org/10.1016/j.nima.2007.05.090

Hurtado-Bermúdez S, Valencia JM, Rivera-Silva J, Mas JL, Aparicio I, Santos JL, Alonso E (2019) Levels of radionuclide concentrations in benthic invertebrate species from the Balearic Islands, Western Mediterranean, during 2012–2018. Mar Pollut Bull 149. https://doi.org/10.1016/j.marpolbul.2019.110519

Iurian AR, Pitois A, Kis-Benedek G, Migliori A, Padilla-Alvarez R, Ceccatelli A (2016) Assessment of measurement result uncertainty in determination of 210Pb with the focus on matrix composition effect in gamma-ray spectrometry. Appl Radiat Isot 109:61–69. https://doi.org/10.1016/j.apradiso.2015.11.067

Ivanovich M, Harmon RS (eds) (1992) Uranium-series disequilibrium: applications to earth, marine, and environmental sciences, 2nd edn. Clarendon Press, Oxford

Ketterer ME, Szechenyi SC (2008) Determination of plutonium and other transuranic elements by inductively coupled plasma mass spectrometry: a historical perspective and new frontiers in the environmental sciences. Spectrochim Acta Part B at Spectrosc 63(7):719–737. https://doi.org/10.1016/j.sab.2008.04.018

Ketterer ME, Watson BR, Matisoff G, Wilson CG (2002) Rapid dating of recent aquatic sediments using Pu activities and240Pu/239Pu as determined by quadrupole inductively coupled plasma mass spectrometry. Environ Sci Technol 36(6):1307–1311. https://doi.org/10.1021/es010826g

Kosmas C, Danalatos N, Cammeraat LH, Chabart M et al (1997) The effect of land use on runoff and soil erosion rates under Mediterranean conditions. CATENA 29(1):45–59. https://doi.org/10.1016/S0341-8162(96)00062-8

Koulouri M, Chr G (2007) Land abandonment and slope gradient as key factors of soil erosion in Mediterranean terraced lands. CATENA 69(3):274–281. https://doi.org/10.1016/j.catena.2006.07.001

Lang A, Bork HR (2006) Past soil erosion in Europe. In: Boardman J, Poesen J (eds) Soil erosion in Europe, Wiley-Interscience, Hoboken, NJ, USA. https://doi.org/10.1002/0470859202.ch35

Legarda F, Romero LM, Herranz M, Barrera M, Idoeta R, Valiño F et al (2011) Inventory and vertical migration of 137Cs in Spanish mainland soils. J Environ Radioact 102(6):589–597. https://doi.org/10.1016/j.jenvrad.2011.03.007

Lépy MC, Altzitzoglou T, Anagnostakis MJ, Capogni M et al (2012) Intercomparison of methods for coincidence summing corrections in gamma-ray spectrometry-part II (volume sources). Appl Radiat Isot 70(9):2112–2118. https://doi.org/10.1016/j.apradiso.2012.02.079

López-Coto I, Mas JL, Bolivar JP (2013) A 40-year retrospective European radon flux inventory including climatological variability. Atmospheric Environ 73:22–33. https://doi.org/10.1016/j.atmosenv.2013.02.043

Lozano RL, Hernández-Ceballos MA, Rodrigo JF (2013) San Miguel Mesoscale behavior of 7Be and 210Pb in superficial air along the gulf of Cadiz (south of Iberian Peninsula). Atmospheric Environ 80:75–84. https://doi.org/10.1016/j.atmosenv.2013.07.050

Lozano RL, San Miguel EG, Bolívar JP, Baskaran M (2011) Depositional fluxes and concentrations of 7Be and 210Pb in bulk precipitation and aerosols at the interface of Atlantic and Mediterranean coasts in Spain. J Geophys Res Atmos 116(18):D18213. https://doi.org/10.1029/2011JD015675

Mabit L, Benmansour M, Abril JM, Walling DE et al (2014) Fallout210Pb as a soil and sediment tracer in catchment sediment budget investigations: a review. Earth Sci Rev 138:335–351. https://doi.org/10.1016/j.earscirev.2014.06.007

Mabit L, Bernard C, Lee Zhi Yi A, Fulajtar E, Dercon et al (2018) Promoting the use of isotopic techniques to combat soil erosion: an overview of the key role played by the SWMCN Subprogramme of the Joint FAO/IAEA Division over the last 20 years. Land Degrad Dev 29(9):3077–3091. https://doi.org/10.1002/ldr.3016

Mabit L, Chhem-Kieth S, Toloza A, Vanwalleghem T, Bernard C, Amate JI et al (2012) Radioisotopic and physicochemical background indicators to assess soil degradation affecting olive orchards in southern Spain. Agric Ecosys Environ 159:70–80. https://doi.org/10.1016/j.agee.2012.06.014

Mabit L, Meusburger K, Fulajtar E, Alewell C (2013) The usefulness of137Cs as a tracer for soil erosion assessment: a critical reply to Parsons and Foster (2011). Earth Sci Rev 127:300–307. https://doi.org/10.1016/j.earscirev.2013.05.008

Menéndez-Duarte R, Fernández S, Soto J (2009) The application of 137Cs to post-fire erosion in north-west Spain. Geoderma 150(1–2):54–63. https://doi.org/10.1016/j.geoderma.2009.01.012

Meusburger K, Mabit L, KettererME PJH, Sandor T, Porto P, Alewell C (2016) A multi-radionuclide approach to evaluate the suitability of 239 + 240Pu as soil erosion tracer. Sci Total Environ 566–567:1489–1499. https://doi.org/10.1016/j.scitotenv.2016.06.035

Meusburger K, Porto P, Mabit L, La Spada C, Arata L, Alewell C (2018) Excess lead-210 and plutonium-239+240: two suitable radiogenic soil erosion tracers for mountain grassland sites. Environ Res 160:195–202. https://doi.org/10.1016/j.envres.2017.09.020

Ministerio de Agricultura, Pesca y Alimentación España (2008) Inventario nacional erosión suelos 2002–2012. Madrid: Dirección General para la Biodiversidad. https://www.miteco.gob.es/es/

biodiversidad/temas/inventarios-nacionales/libro28_ines_madrid_tcm30-154003.pdf. Accessed 16 Jan 2023
Montgomery DR (2007) Soil erosion and agricultural sustainability. Proc Natl Acad Sci USA 104:13268–13272. https://doi.org/10.1073/pnas.0611508104
Moreira JM (1995) Reconocimiento biofísico de espacios naturales protegidos: Parque Natural Sierra de Hornachuelos (Consejería de Medio Ambiente Andalucía). Junta de Andalucía. https://www.juntadeandalucia.es/medioambiente/portal/documents/20151/5395847/reconocimiento_biofisico_hornachuelos.pdf/29eb7ac8-131c-3ee8-9051-83a4d808d257?t=1619780778518. Accessed 16 Jan 2023
Navas A, Quine TA, Walling DE, Gaspar L, Quijano L, Lizaga I (2017) Relating intensity of soil redistribution to land use changes in abandoned pyrenean fields using fallout caesium-137. Land Degrad Dev 28(7):2017–2029. https://doi.org/10.1002/ldr.2724
Panagos P, Borrelli P, Poesen J, Ballabio C, Lugato E, Meusburger K et al (2015) The new assessment of soil loss by water erosion in Europe. Environ Sci Policy 54:438–447. https://doi.org/10.1016/j.envsci.2015.08.012
Panagos P, Meusburger K, Ballabio C, Borrelli P, Alewell C (2014) Soil erodibility in Europe: a high-resolution dataset based on LUCAS. Sci Total Environ 479–480(1):189–200. https://doi.org/10.1016/j.scitotenv.2014.02.010
Parsons AJ, Foster IDL (2011) What can we learn about soil erosion from the use of137Cs? Earth Sci Rev 108(1–2):101–113. https://doi.org/10.1016/j.earscirev.2011.06.004
Parsons AJ, Foster IDL (2013) The assumptions of science. A reply to Mabit et al. (2013). Earth Sci Rev 127:308–310. https://doi.org/10.1016/j.earscirev.2013.05.011
Porto P, Walling DE, Callegari GE, La Spada C (2012) Further investigation of the relationship between 137Cs and 210Pbex flux and sediment output from two small experimental catchments in Calabria, southern Italy. IAHS-AISH Publication 356:385–393. https://iahs.info/uploads/dms/15834.57-385-393-356-23-ICCE2012_Paolo-Porto--30--revised.pdf. Accessed 21 Jan 2023
Raab G, Scarciglia F, Norton K, Dahms D, Brandová D, de Castro PR et al (2018) Denudation variability of the Sila Massif upland (Italy) from decades to millennia using 10Be and 239+240Pu. Land Degrad Dev 29(10):3736–3752. https://doi.org/10.1002/ldr.3120
Rosa D de la, Moreno CB, Gómez JLM, Barahona E, Madueño JMM, Gago R et al (1984) Catálogo de suelos de Andalucía. Retrieved from https://www.juntadeandalucia.es/medioambiente/documentos_tecnicos/catalogo2/catalogo_ind.html. Accessed 15 Jan 2023
Salminen T (2006) Geochemical atlas of Europe part 1: background information, methodology and maps. In: Salminen, T. (Ed.). Geochemical Atlas of Europe, vol. 1. EuroGeosurveys and Foregs, Espoo, Finland
Sanchez-Cabeza JA, Garcia-Talavera M, Costa E, Peña V, Garcia-Orellana J, Masqué P, Nalda C (2007) Regional calibration of erosion radiotracers (210Pb and 137Cs): atmospheric fluxes to soils (northern Spain). Environ Science Technol 41(4):1324–1330. https://doi.org/10.1021/es061356z
Sanders CJ, Santos IR, Maher DT, Breithaupt JL et al (2016) Examining 239+240Pu, 210Pb and historical events to determine carbon, nitrogen and phosphorus burial in mangrove sediments of Moreton Bay, Australia. J Environ Radioact 151:623–629. https://doi.org/10.1016/j.jenvrad.2015.04.018
Schlesinger WH (2021) Some thoughts on the biogeochemical cycling of potassium in terrestrial ecosystems. Biogeochemistry 154:427–432. https://doi.org/10.1007/s10533-020-00704-4
Taguas EV, Ayuso JL, Peña A, Yuan Y, Pérez R (2009) Evaluating and modelling the hydrological and erosive behaviour of an olive orchard microcatchment under no-tillage with bare soil in Spain. Earth Surf Proces Landf 34(5):736–751. https://doi.org/10.1002/esp.1775
Taguas EV, Carpintero E, Ayuso JL (2013) Assessing land degradation risk through the long-term analysis of erosivity: a case study in Southern Spain. Land Degrad Dev 24(2):179–187. https://doi.org/10.1002/ldr.1119
Tims SG, Everett SE, Fifield LK, Hancock GJ, Bartley R (2010) Plutonium as a tracer of soil and sediment movement in the Herbert River, Australia. Nucl Instrum Methods Phys Res B 268(7–8):1150–1154. https://doi.org/10.1016/j.nimb.2009.10.121
UNSCEAR (2000) Report of the United Nations Scientific Committee on the Effects of Atomic Radiation. United Nations, New York
Vaca F, Manjón G, García-León M (2001) The presence of some artificial and natural radionuclides in a Eucalyptus forest in the south of Spain. J Environ Radioact 56(3):309–325. https://doi.org/10.1016/S0265-931X(00)00211-3
Vidmar T, Aubineau-Laniece I, Anagnostakis MJ, Dv A et al (2008) An intercomparison of Monte Carlo codes used in gamma-ray spectrometry. Appl Radiat Isot 66(6–7):764–768. https://doi.org/10.1016/j.apradiso.2008.02.015
Xu Y, Qiao J, Pan S, Hou X, Roos P, Cao (2015) Plutonium as a tracer for soil erosion assessment in northeast China. Sci Total Environ 511:176–185. https://doi.org/10.1016/j.scitotenv.2014.12.006

Authors and Affiliations

A. Peñuela[1] · S. Hurtado[2] · V. García-Gamero[1] · J. L. Mas[3] · M. E. Ketterer[4] · T. Vanwalleghem[1] · J. A. Gómez[5]

✉ J. L. Mas
ppmasb@us.es

[1] Department of Agronomy, University of Córdoba, Edif. Da Vinci, Ctra. Madrid Km 396, 14071 Córdoba, Spain

[2] Dpto. Física Aplicada II, Universidad de Sevilla. ETS Arquitectura, Avda. Reina Mercedes 2, 41012 Seville, Spain

[3] Dpto. Física Aplicada I, Universidad de Sevilla, ETSI-Informática, Avda. Reina Mercedes S/N, 41012 Seville, Spain

[4] Chemistry and Biochemistry, Northern Arizona University, Flagstaff, AZ 86011-5698, USA

[5] Institute for Sustainable Agriculture (IAS-CSIC), Agronomy Department, Avenida Menéndez Pidal S/N, 14004 Córdoba, Spain